2008

Thevenin Equivalent Circuit Estimation and Application for Power System Monitoring and Protection

Mohammad M. Iftakhar
University of Kentucky

ABSTRACT OF THESIS

Thevenin Equivalent Circuit Estimation and Application for Power System Monitoring and Protection

The Estimation of Thevenin Equivalent Parameters is useful for System Monitoring and Protection. We studied a method for estimating the Thevenin equivalent circuits. We then studied two applications including voltage stability and fault location. A study of the concepts of Voltage Stability is done in the initial part of this thesis. A Six Bus Power System Model was simulated using MATLAB SIMULINK®. Subsequently, the Thevenin Parameters were calculated. The results were then used for two purposes, to calculate the Maximum Power that can be delivered and for Fault Location.

KEYWORDS: Thevenin Equivalent Circuit, Voltage Stability, Rotor Angle Stability, Fault Location, Power System Monitoring

Mohammad M Iftakhar
December 31st 2008

Thevenin Equivalent Circuit Estimation and Application for Power System Monitoring and Protection

By

Mohammad Museb Iftakhar

_____

(Director of Thesis)

_____

(Director of Graduate Studies)

_____

(Date)

RULES FOR THE USE OF THESIS

Unpublished thesis submitted for the Master's degree and deposited in the University of Kentucky Library are as a rule open for inspection, but are to be used only with due regard to the rights of the authors. Bibliographical references may be noted, but quotations or summaries of parts may be published only with the permission of the author, and with the usual scholarly acknowledgments.

Extensive copying or publication of the dissertation in whole or in part also requires the consent of the Dean of the Graduate School of the University of Kentucky.

A library that borrows this dissertation for use by its patrons is expected to secure the signature of each user.

Name Date

_____
_____
_____
_____
_____
_____
_____
_____
_____
_____
_____
_____
_____
_____
_____
_____
_____
_____
_____

THESIS

Mohammad Museb Iftakhar

The Graduate School
University of Kentucky
2009

Thevenin Equivalent Circuit Estimation and Application for Power System Monitoring and Protection

---

THESIS

A thesis submitted in partial fulfillment of the requirements for the degree of Master of Science in the College of Engineering at the
University of Kentucky

By
Mohammad Museb Iftakhar
Lexington, Kentucky
Director: Dr. Yuan Liao, Department of Electrical and Computer Engineering
Lexington, Kentucky
2009

Dedicated to My Parents, Brothers and Sister

ACKNOWLEDGEMENTS

I would like to take this opportunity to express my sincere thanks and heartfelt gratitude to my academic advisor and thesis chair Dr. Yuan Liao for his guidance and support throughout my thesis. I am very thankful for his constant encouragement during the thesis. Without him the thesis would have never taken its present shape. I am greatly indebted for his support.

My parents and my siblings have been great sources of support throughout my studies. My friends have given me a lot of love without which this work would not have been possible.

I also would like to extend my thanks to Dr. Paul A Dolloff and Dr. Jimmy J Cathey for serving on my thesis committee and providing me with invaluable comments and suggestions for improving this thesis.

Table of Contents

List of Tables

List of Figures

1. Introduction

1.1 Background

The pressure on the power transmission network has been increasing in recent times. Some of the reasons for this which have been mentioned in [1] are

- A deregulated energy market.
- Environmental constraints.
- Limited investment in transmission system reinforcement.
- An increased competition in order to yield greater outputs.

Hence, the Power System is forced to operate closer to the stability limit. A Major problem arising out of this is voltage instability or collapse, which causes a steady state security problem. When the loading of a Power system approaches the maximum permissible loading, at some local bus in the power transmission network, the magnitude of the voltage tends to decrease. But only by knowing the voltage magnitude of local buses, we cannot exactly assess the impending voltage collapse. The voltage magnitude decreases because of inadequate local reactive power support to meet local demand and losses. Large amounts of reactive power from other buses in the network will deteriorate the voltage profile which may lead to voltage collapse.

In recent years, voltage instability has been responsible for major blackouts. The following are some examples [7]:

- North East blackout, August 14, 2003.
- Texas blackout, September 13, 2008.
- New York Power Pool Disturbances of September 22, 1970
- Florida System Disturbance of December 28, 1982
- French System Disturbances of December 19, 1978 and January 12, 1987
- Northern Belgium System Disturbance of August 4, 1982
- Swedish System Disturbance of December 27, 1983
- Japanese System Disturbance of July 23, 1987.

Thus voltage stability studies have become of more importance than ever.

Another important thing to consider in this thesis is fault location. Fault location studies are very important for the transient stability limit of the system. The increased complexities of modern power systems have raised the importance of fault location research studies [11]. Accurate and fast fault location helps in reducing the maintenance and restoration times, reduce the outage times and thus improve the power system reliability [12].

1.2 Purpose of the Thesis

To operate the power system with an adequate security margin, it is essential to estimate the maximum permissible loading [1].The maximum power that can be transferred to the load bus in a power system can be effectively studied by estimating the Thevenin equivalent circuit of the power system Model. Thus, in one part of my Thesis, I will be calculating the Thevenin parameters of a six bus power system model. This would provide me with considerable results to calculate the maximum power that can be delivered. The Thevenin equivalent circuit parameters are useful in the applications for power system monitoring and protection. The Thevenin parameters that I obtain in the first part are used for fault location based on voltage measurements. The fault location algorithm is taken from [5], which are described in detail in Chapter 4.

1.3 Overview of System Stability

The stability of a system of interconnected dynamic components is its ability to return to normal or stable operation after having been subjected to some form of disturbance [8]. In a power system, we typically deal with two forms of instability: The loss of synchronism between synchronous machines and voltage instability. Synchronous stability can be classified as steady state and transient stability and are studied in this chapter. The voltage stability is studied in the next chapter. The equations and figures in the subsequent sections have mainly been obtained from [4] and [8].

As defined in [8], steady state stability is the ability of the power system, when operating under given load conditions, to retain synchronism when subjected to small disturbances

such as the continual changes in load or generation and the switching out of lines. This is also known as dynamic stability.

Transient stability deals with sudden and large changes in the system. One example is faults in a Power system. During fault conditions, the stability limit is less than the steady state condition. Before we make a detailed study of steady state and transient stability, it is important to study the equation of motion of a rotating machine.

1.4 Equation of Motion of a Rotating Machine

In this section, we will be studying the Equation of Motion of a Rotating Machine and deriving the swing equation. The equations in this section have all been obtained from [8].

Let the moment of inertia of the rotor be I and the angular acceleration is α. ΔT is the net torque applied on the rotor. ω is the synchronous speed of the rotor (radians/second).

The kinetic energy absorbed by the rotor is given by $\frac{1}{2}I\omega^2$ Joules.

The angular momentum is $M = I\omega$ Joules-Seconds per radian. An inertia constant, H can be defined as the stored energy at synchronous speed per volt-ampere of the rating of the machine [8]. As we know that the unit of energy used in power systems analysis is Kilojoules or Mega joules and if we consider the rating of the machine to be G Mega-Volt-Amperes, then by multiplying G with the inertia constant we get the kinetic energy of the machine.

$GH = \frac{1}{2}I\omega^2 = \frac{1}{2}M\omega$ is the Kinetic Energy or the stored Energy. (1.1)

$\omega = 360 f$ Electrical Degrees per second where f is the system frequency in Hz. (1.2)

Substituting (1.2) in (1.1)

$$GH = \frac{1}{2}M(360)f \tag{1.3}$$

$$\Rightarrow M = GH/180f \text{ Mega joule-seconds/electrical degree} \tag{1.4}$$

$\Delta T =$ Mechanical Torque Input- Electrical Torque Output

$$= I\frac{d^2\delta}{dt^2} \tag{1.5}$$

$$\therefore \frac{d^2\delta}{dt^2} = \frac{\Delta T}{I} = \frac{(\Delta T\omega)\omega}{2xI\omega^2/2} \tag{1.6}$$

$$= \frac{\Delta P.\omega}{2xK.E.} \tag{1.7}$$

Here $\Delta P = P_{mech} - P_{electrical}$ (1.8)

By using Equation (1.1) in (1.7), we can write

$$\frac{d^2\delta}{dt^2} = \frac{\Delta P}{M} \tag{1.9}$$

There is an increase in the value of δ when there is a negative change in the Power output in Equation (1.9). $\Delta P = P_{mech} - P_{electrical}$ is sometimes considered as the change in Electrical Power output. An increase in $\Delta P_{electrical}$ will increase the value of δ. The Power input is assumed to be constant.

$$\Rightarrow \frac{d^2\delta}{dt^2} = -\frac{\Delta P}{M} \text{ or } M\frac{d^2\delta}{dt^2} + \Delta P = 0 \tag{1.10}$$

Equation (1.10) is known as Swing Equation.

Now that we have studied about the Equation of Motion of Rotating Machine, we can analyze Steady State and Transient Stability of a System based on this.

1.5 Steady State Stability

In this section we will be studying the steady state analysis for a power system. The equations in this section have been obtained from [4]. The steady state stability limit of a particular circuit of a power system is defined as the maximum power that can be transmitted to the receiving end without loss of synchronism [4].Figure 1.1[4] represents a simple system for the purpose of analysis.

The dynamics of this system are described by the equations (1.11) to (1.13)

$$M\frac{d^2\delta}{dt^2} = P_m - P_e \tag{1.11}$$

$$M = \frac{H}{\pi f} \text{ in the Per Unit System} \tag{1.12}$$

$$P_e = \frac{|E||V|}{X_d} \sin\delta = P_{\max} \sin\delta \tag{1.13}$$

X_d is the direct axis reactance . The plot for equation (1.13) also known as the power angle curve is represented in Figure 1.2[4]

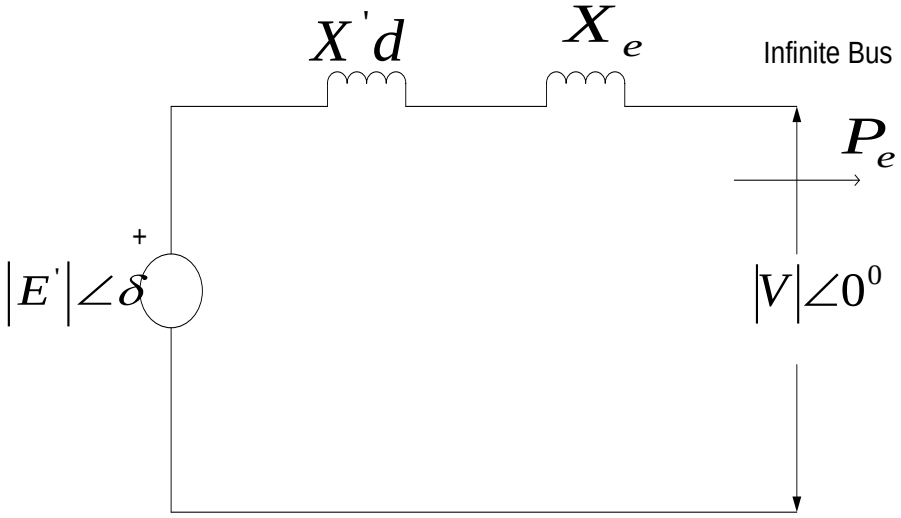

Figure 1.1 Machine Connected to Infinite Bus

The system has a steady power transfer $P_{eo} = P_m$ and the torque angle is δ_o as shown in Figure 1.2. For a small increment ΔP in the electric power with the input P_m being constant, the torque angle changes to $(\delta_o + \Delta\delta)$. Linearizing about the operating point $Q_o(P_{eo}, \delta_o)$ [4], we get

$$\Delta P_e = \left(\frac{\partial P_e}{\partial \delta}\right)_0 \Delta\delta \tag{1.14}$$

Rewriting Equation (1.11) in the current analysis,

$$M\frac{d^2\Delta\delta}{dt^2} = P_m - (P_{eo} + \Delta P_e) = -\Delta P_e \tag{1.15}$$

Using Equation (1.14) in (1.15)

$$M\frac{d^2\Delta\delta}{dt^2} + \left[\frac{\partial P_e}{\partial \delta}\right]_0 \Delta\delta = 0 \tag{1.16}$$

$$\Rightarrow \left[Mk^2 + \left(\frac{\partial P_e}{\partial \delta}\right)_0\right]\Delta\delta = 0 \tag{1.17}$$

Where $k = \frac{d}{dt}$

The stability of the system for small changes is determined by the characteristic equation

[4] $$\left[Mk^2 + \left(\frac{\partial P_e}{\partial \delta} \right)_0 \right] = 0 \qquad (1.18)$$

The roots of Equation (1.18) are given by

$$k = \pm \left[\frac{-\left(\partial P_e / \partial \delta \right)_0}{M} \right]^{\frac{1}{2}} \qquad (1.19)$$

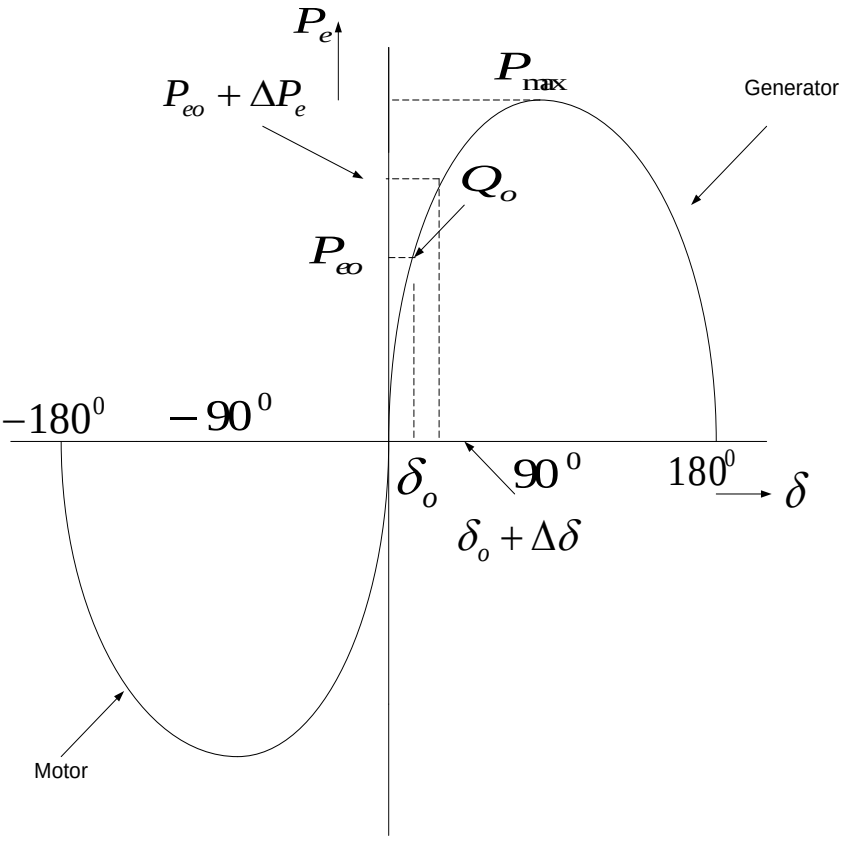

Figure 1.2 Power Angle Curve

Now the system behavior depends on the value of $(\partial P_e / \partial \delta)_0$.

If $(\partial P_e / \partial \delta)_0$ is positive, the roots are imaginary and conjugate. The system behavior is oscillatory about δ_o. But in our analysis the machine damper windings line resistance had

been neglected. These cause the system oscillations to decay and hence the system is stable for a small increment in power.

If $(\partial P_e / \partial \delta)_0$ is negative, the roots are real. One is positive and the other is negative. Though, they are equal in magnitude. For a small increment in power, the system is unstable as the synchronism is lost due to increase in torque angle with increase in power.

From Equation (1.13) assuming $|E|, |V|$ to remain constant, the system is unstable if $\delta_o > 90^0$. (1.20)

The maximum power transfer without loss of stability occurs for $\delta_o = 90^0$ (1.21)

The maximum power transferred is therefore given by

$$P_{\max} = \frac{|E||V|}{X} \tag{1.22}$$

But in the analysis we had assumed that the internal machine voltage remains constant. In such a case as the loading is increased, the terminal voltage dips heavily which is practically not acceptable. In practice, we must consider the steady state stability limit by assuming that the excitation is adjusted for every load increase to keep the terminal voltage constant. The effects of governor and excitation control were not considered in the analysis.

Steady state stability limit is very important as it should be taken care that a system can operate above transient stability but not above steady state stability limit. The transient stability limit can be made to closely approach the steady state limit currently with increased speeds in fault clearing.

1.6 Methods of Improving Steady State stability Limit

The following methods can be used depending on the conditions in order to improve the steady state stability limit [4]

- From Equation (1.22), we can say that the steady state stability limit can be improved by reducing X or by increasing either E or V or both.
- For transmission lines of high reactance, the stability limit can be increased by using two parallel lines.

- Use of series capacitors in the lines to get better voltage regulation raises the stability limits by decreasing the line reactance.
- Employing quick excitation systems and higher excitation voltages.

1.7 Transient Stability Limit

Transient stability limit is the maximum possible power that can be transmitted through a point in the system when the system is operating with stability during transient disturbances [15]. The type of disturbance and the duration of disturbance affect the transient stability limit. The duration of a fault determines the amount of power that can be transmitted from one machine to another machine in a two machine system without loss of synchronism. The power limit is determined using the Equal Area Criterion. This is studied in section 1.8.

1.8 Equal Area Criterion

As we had considered one finite machine system for analysis for steady state stability, we will study the Equal Area Criterion for one finite machine swinging with an infinite bus in this section. The equations in this section have been mainly obtained from [15]. The detailed study of Equal Area Criterion for a system with two finite machines swinging with respect to each other is discussed in [4] and [15].

The Swing Equation of a finite machine swinging with respect to an infinite machine is given by $M\frac{d^2\delta}{dt^2} = P_m - P_e = P_a$ (1.23)

Multiplying both sides of Equation (1.23) by $2d\delta/dt$ and rearranging, we get

$$2\frac{d^2\delta}{dt^2}\frac{d\delta}{dt} = 2\frac{P_a}{M}\frac{d\delta}{dt} \tag{1.24}$$

$$\Rightarrow \frac{d}{dt}\left[\left(\frac{d\delta}{dt}\right)^2\right] = 2\frac{P_a}{M}\frac{d\delta}{dt} \tag{1.25}$$

Upon integrating Equation (1.25) with respect to time, we get

$$\left[\left(\frac{d\delta}{dt}\right)^2\right] = \frac{2}{M}\int_{\delta_o}^{\delta} P_a d\delta \tag{1.26}$$

$$\Rightarrow \frac{d\delta}{dt} = \omega = \sqrt{\frac{2}{M}\int_{\delta_o}^{\delta} P_a d\delta} \tag{1.27}$$

$\omega = 0$ when the machine comes to rest with respect to the infinite machine. The condition required for the stability of a single machine system connected to infinite bus is

$$\int_{\delta_o}^{\delta} P_a d\delta = 0 \tag{1.28}$$

The integral in Equation (1.28) can be represented as the area between the curve P_m versus δ and the curve P_e versus δ. This is shown in Figure 1.3[15]. For the area to be Zero, $A_1(P_m > P_e) = A_2(P_m < P_e)$ [9]. Hence this method is called Equal Area criterion.

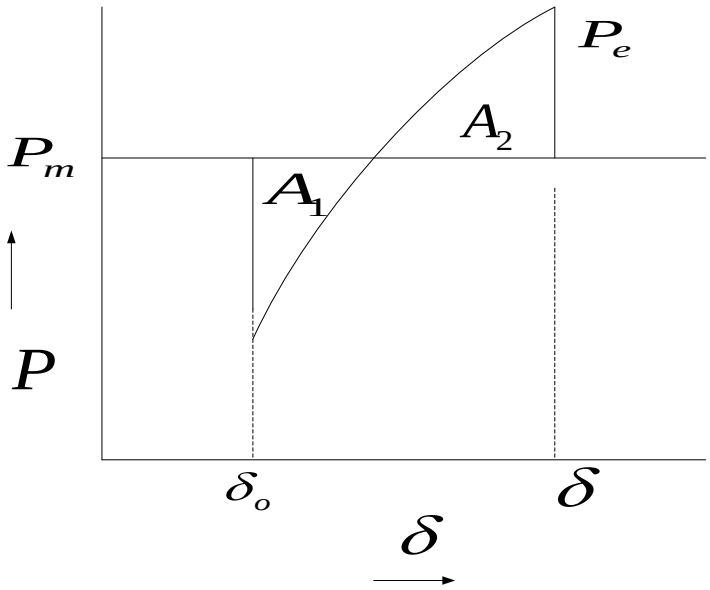

Figure 1.3 Curve Showing the Equal Area criterion

1.9 Factors Affecting Transient Stability

The factors affecting transient stability limit mentioned in [15] are as follows:

- Inertia Constant
- Type of Disturbance
- Fault clearing time

- Location of the fault
- Initial operating Condition of the system
- The way in which the fault is cleared.

Thus, in this chapter we have presented the purpose of the thesis research that has been carried out and an overview of the basic concepts related to the area of my research. An advanced study of these concepts can be made through the references that have been mentioned.

2. Power System Voltage Stability Analysis

In chapter 1, I gave an overview about the importance of voltage stability studies as voltage instability or voltage collapse may lead to a blackout. In this chapter we will be making a detailed study of the relevant concepts that could help us make the understanding of voltage stability better. Before we study voltage stability in particular, we define and classify power system stability in general. This is studied in the initial sections of this chapter. In the later sections we discuss voltage stability. These include the definitions, concepts of mathematical formulation of the voltage stability problems and some significant criteria of voltage stability studies. The equations and figures have been mainly obtained from [2] and [4].

2.1 Definition and Classification of Power System stability

In a broad terminology, power system stability may be defined as that property of the power system that enables it to remain in a state of operating equilibrium under normal operating conditions and to regain an acceptable state of equilibrium after being subjected to a disturbance [2]. The definitions of power system stability though have not been precise and do not include all practical instability scenarios [3]. A proposal is presented in [3] which attempts to define power system stability more precisely which includes all forms of system instability. “Power system stability is the ability of an electric power system, for a given initial operating condition, to regain a state of operating equilibrium after being subjected to a physical disturbance with most system variables bounded so that practically the entire system remains intact” [3].

2.2 Classification of Power System Stability

Power system stability is classified based on the following considerations [2]

- The physical nature of the instability
- The size of the disturbance
- The time span

Based on the physical nature of the instability, it can be classified as rotor angle stability and voltage stability. Based on the size of the disturbance, it is classified as large disturbance and small disturbance stability. Based on the time span, it can be classified as long term and short term stability.

2.3 Voltage Stability

Voltage stability is the ability of a power system to maintain steady acceptable voltages at all buses in the system under normal operating conditions and after being subjected to a disturbance [2]. There is voltage instability when there is voltage drop in the system or at a bus due to several reasons which include a general disturbance, a change in system condition or due to fluctuating loads. But the main reason for a voltage instability is the inadequacy of reactive power demands to be met by the system.

Reactive power is injected into the system to meet the increasing demands. For a voltage stable system, as the reactive power is injected into the buses in the system, the voltage magnitude should increase. But, if the voltage magnitude decreases even at one bus in the system for increase in reactive power, the System is said to be voltage unstable.

Voltage instability is a local phenomenon but its consequences may have a widespread impact [2]. Voltage instability leads to low voltage profile in the system and it can have a cumulative effect ultimately leading to voltage collapse.

2.4 Voltage Stability Analysis

In this section we study a voltage study analysis for a simple two terminal network. Figure 2.1[2] represents a simple radial system. This figure and the equations in this section are taken from [2].

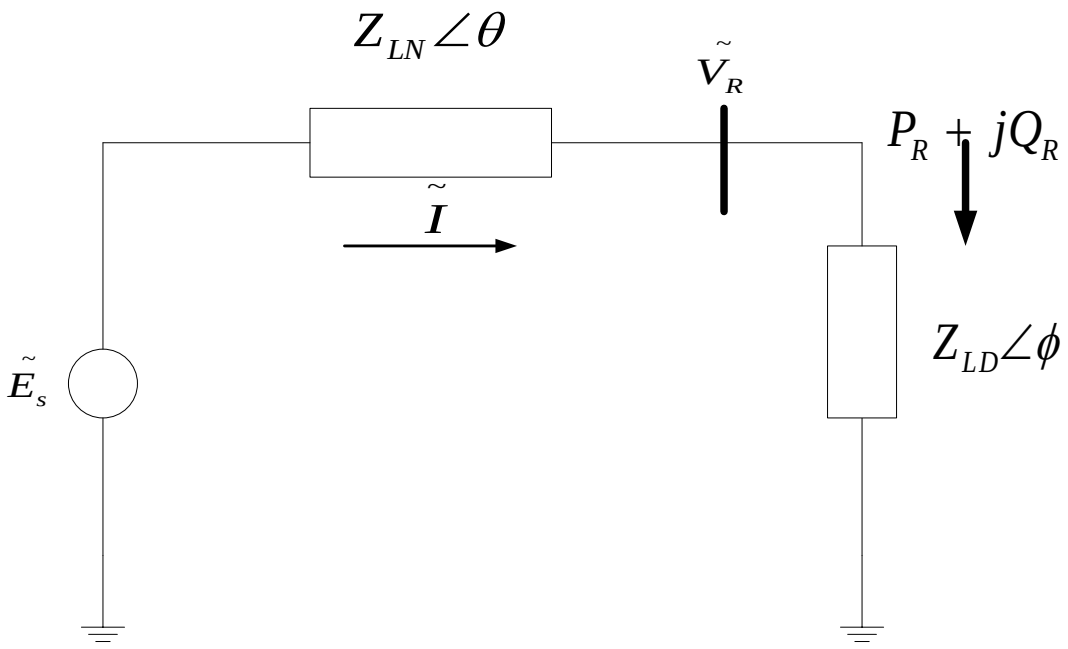

Figure 2.1 Simple radial System for Voltage Stability Analysis

E_s is the Voltage Source

Z_{LD} is the load impedance

Z_{LN} is the series impedance of the system .

The Current $\tilde{I}$ can be expressed as

$$\tilde{I} = \frac{\tilde{E}_s}{\tilde{Z}_{LN} + \tilde{Z}_{LD}} \tag{2.1}$$

$\tilde{I}$ and $\tilde{E}_s$ are the phasors of current and source voltage.

The series impedance and the load impedance phasors can be expressed as

$\tilde{Z}_{LN} = Z_{LN}\angle\theta$ and $\tilde{Z}_{LD} = Z_{LD}\angle\phi$ respectively. (2.2)

The magnitude of the current can then be expressed as

$$|I| = \frac{E_s}{\sqrt{\left(Z_{LN}\cos\theta + Z_{LD}\cos\phi\right)^2 + \left(Z_{LN}\sin\theta + Z_{LD}\sin\phi\right)^2}} \tag{2.3}$$

Simplifying Equation (2.3)

$$|I| = \frac{1}{\sqrt{Z^{'}}} \frac{E_s}{Z_{LN}} \tag{2.4}$$

Where

$$Z^{'} = 1 + \left(\frac{Z_{LD}}{Z_{LN}}\right)^2 + 2\left(\frac{Z_{LD}}{Z_{LN}}\right)\cos(\theta - \phi) \tag{2.5}$$

The Magnitude of Voltage at the receiving end can be expressed as

$$V_R = Z_{LD}|I| \tag{2.6}$$

Substituting the value of current from Eq. (2.4) into Eq. (2.6)

$$= \frac{1}{\sqrt{Z^{'}}} \frac{Z_{LD}}{Z_{LN}} E_s \tag{2.7}$$

Now, calculating the power delivered

It is given by

$$P_R = V_R|I|\cos\phi \tag{2.8}$$

$$= \frac{Z_{LD}}{Z^{'}}\left(\frac{E_s}{Z_{LN}}\right)^2 \cos\phi \tag{2.9}$$

Figure 2.2[2] shows the plots of I, V_R and P_R as a function of Z_{LN} / Z_{LD}. P_R increases rapidly as the load demand i.e. Z_{LN} / Z_{LD} is increased. This is done by decreasing Z_{LD}. P_R reaches a maximum value and then begins to decrease. The maximum value of P_R indicates the maximum value of active power that can be transmitted through an impedance from a constant voltage source. This power transmitted is maximum when the voltage drop in the line is equal in magnitude to V_R that is when $Z_{LN} / Z_{LD} = 1$[2]. With a gradual decrease in Z_{LD} there is an increase in I and decrease in V_R. The reason for a rapid increase in P_R initially is due to the dominant increase of I in comparison to the decrease in V_R at high values of Z_{LD}. As Z_{LD} approaches Z_{LN} this effect is not so dominant and hence there is a gradual change rather than a sharp increase and decrease in the values of I and V_R respectively. As Z_{LD} goes below Z_{LN}, the decrease in V_R dominates the increase in I and hence there is a decrease in P_R.

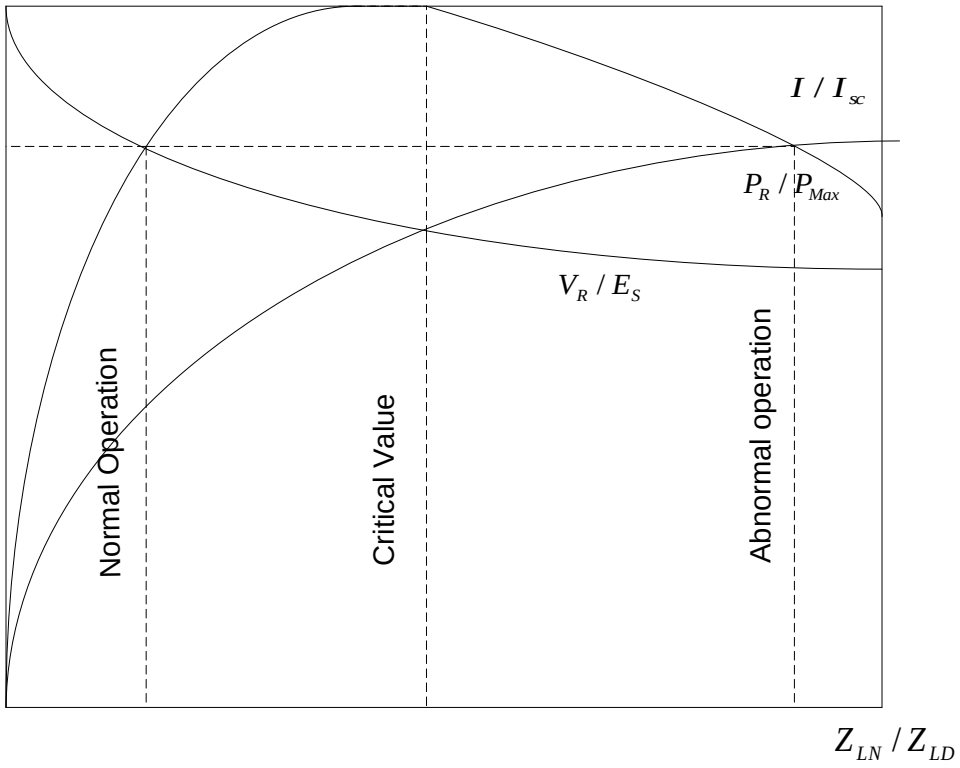

Figure 2.2 Reactive End Voltages, Power and Current as a Function of Load Demand

The normal operation takes place till the critical value is reached. This corresponds to the maximum power in the Figure 2.2. As the load demand increases i.e. as Z_{LN} / Z_{LD} is increasing the control of power would be unstable. This means that as the load impedance Z_{LD} is decreased the power is also reduced. The load characteristics determine if the voltage collapse takes place or not. For a constant impedance static load characteristics, the system stabilizes at power and voltage levels lower than the desired values where as for a constant power load characteristic the system becomes unstable through collapse of load bus voltage [2]. Thus it is important to analyze the relationship between P_R and V_R for the purpose of voltage stability studies.

2.5 P-V Curves

The relationship between P_R and V_R is shown in Figure2.3 [2] for a particular power factor value. But the voltage drop in the transmission lines is a function of both the active and the reactive power transfer as seen in Equations (2.7) and (2.9). Thus the load power factor affects the power voltage characteristics of the system Figure 2.4[2] represents the curves for P_R and V_R for different load power factor values.

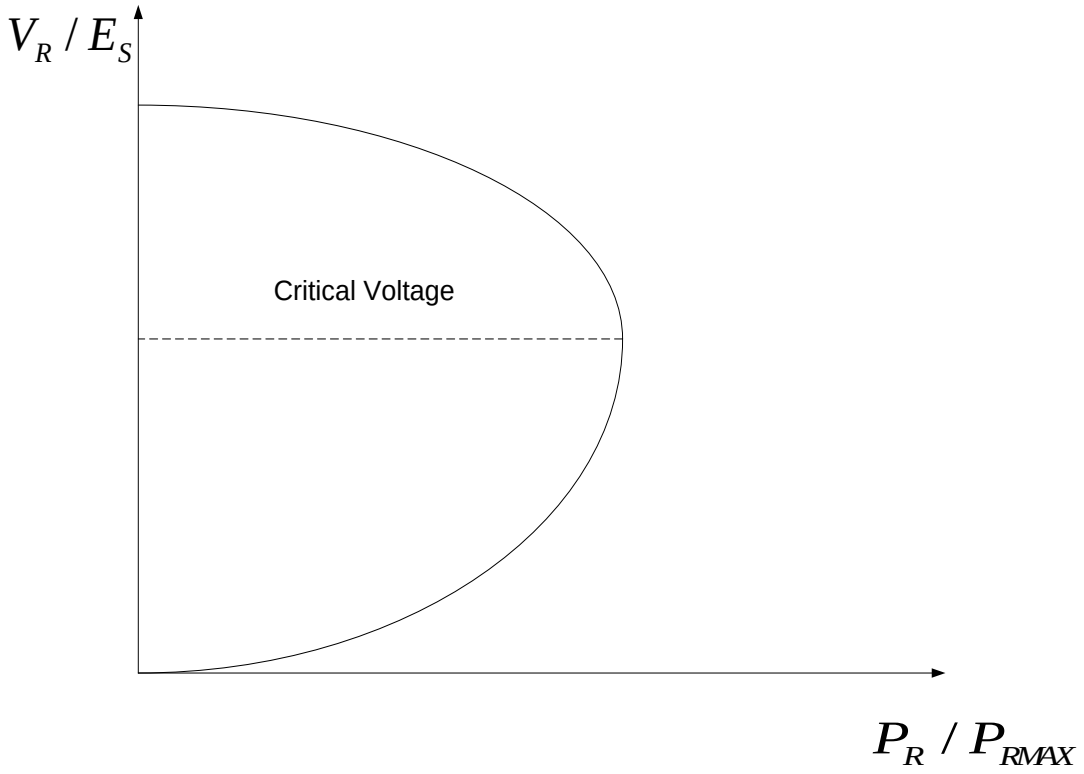

Figure 2.3 Power Voltage Characteristics for the System of Figure2.1

The dotted lines represent the locus of critical operating points. This means that operating points above the critical values represent satisfactory operation. A sudden reduction in power factor, which causes an increase in the reactive power delivered, can cause the system to change from a stable operating condition to an unstable condition as shown in the lower part of the curves in Figure 2.3 and Figure 2.4.

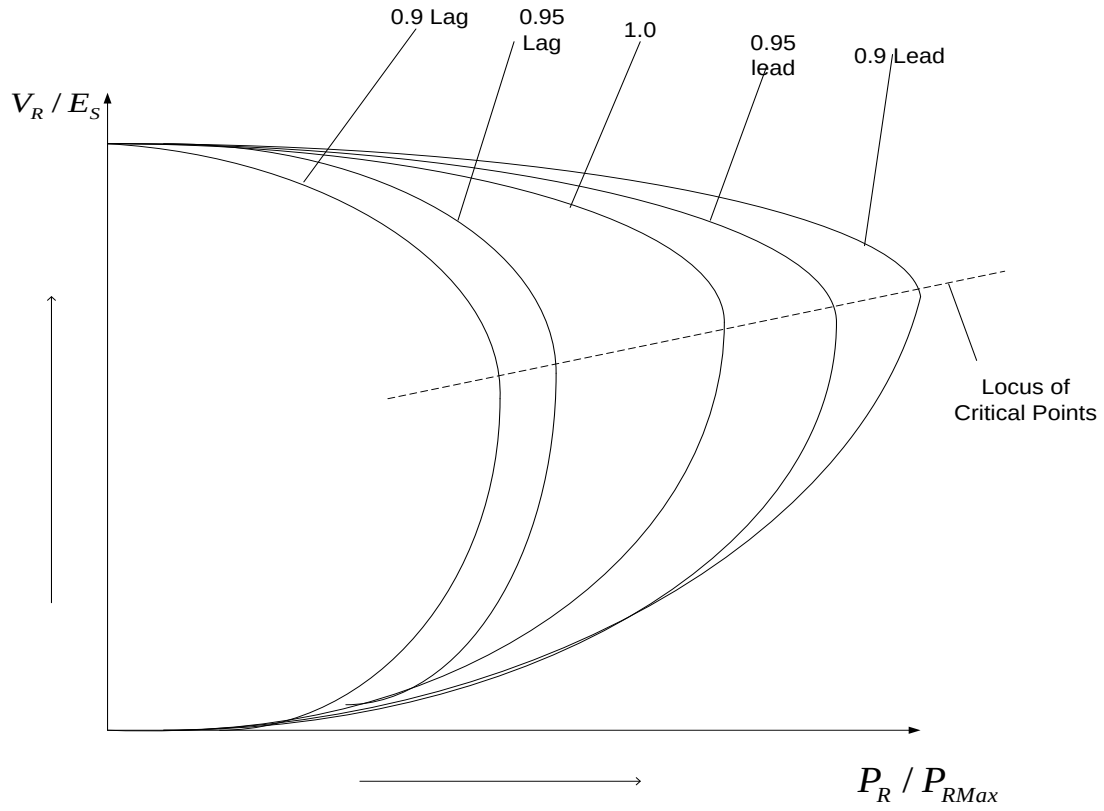

Figure 2.4 Power Voltage characteristics for Different Load Power Factors

2.6 V-Q Characteristics

For purpose of analysis let us consider a simple radial system as shown in Figure 2.5[4]. The system load end voltage can be expressed in terms of P, Q as given in [4]

$$V = \left[\frac{-2QX + E^2}{2} \pm \frac{1}{2} \sqrt{\left(2QX - E^2\right)^2 - 4X^2\left(P^2 + Q^2\right)} \right]^{1/2} \tag{2.10}$$

For Reactive Power Flow $X >> R$

i.e. $\phi \approx 90^0$

$$\Rightarrow Q = \frac{EV}{X}\cos\delta - \frac{V^2}{X}\,[4] \tag{2.11}$$

$$\Rightarrow V^2 - EV\cos\delta + QX = 0\,[4] \tag{2.12}$$

$$\frac{dQ}{dV} = \frac{E\cos\delta - 2V}{X}\,[4] \tag{2.13}$$

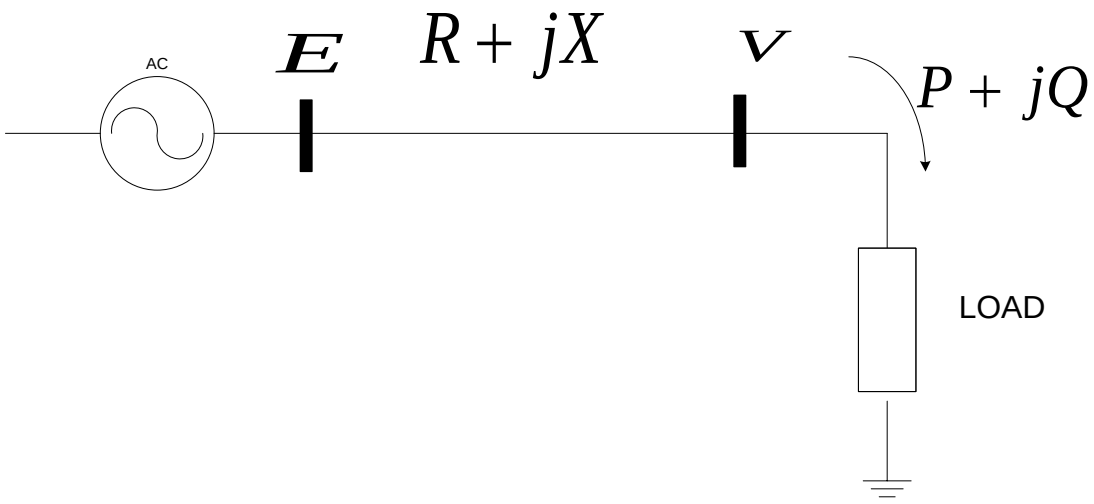

Figure 2.5 Simple Radial Two Bus System

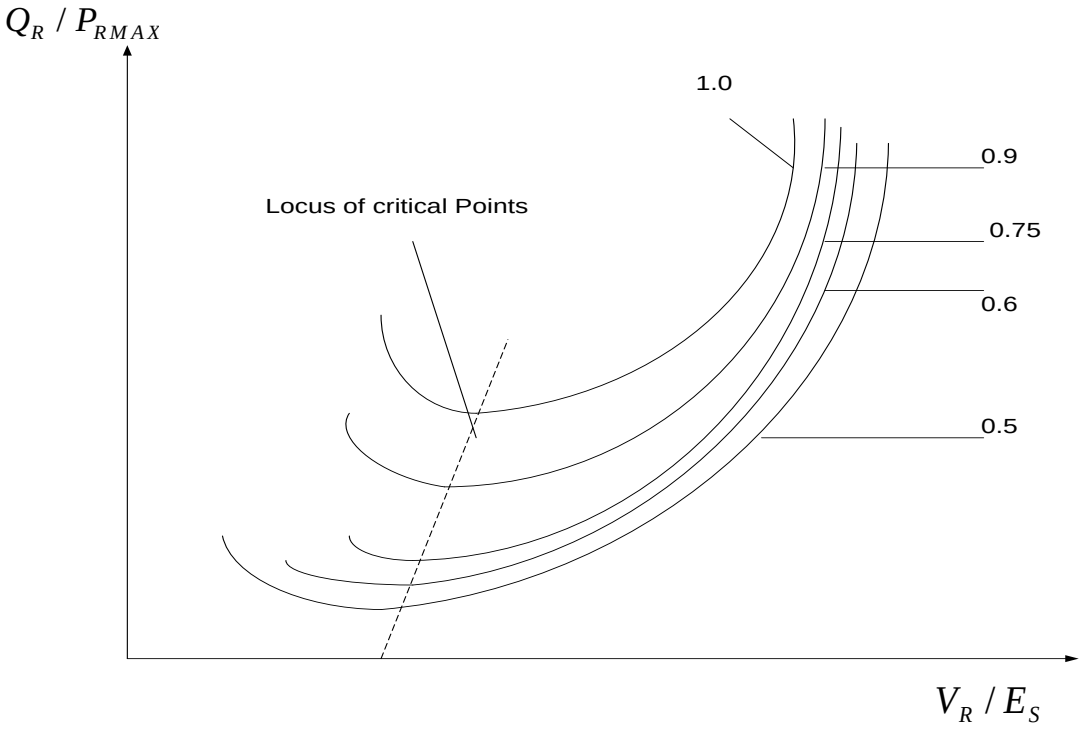

Figure 2.6 V-Q Characteristics of the system in Figure 2.1

Figure 2.6 represents the $V_R - Q_R$ characteristics with different P_R / P_{RMax} ratios of a simple two-terminal system. The system is voltage stable in the region where dQ/dV is positive [4]. The locus of critical operating points is shown in the Figure 2.6 with dotted

lines. The critical operating point is where the voltage stability limit is reached i.e. $dQ/dV = 0$. At voltage stability limit, the limiting reactive power is given by

$$Q_{\lim} = \frac{V^2}{X}\cos 2\delta \text{ [4]} \tag{2.14}$$

The parts of the curve to the right of the minima represent stable operation. There is unstable operation when $dQ/dV < 0$. But stable operation in the region when $dQ/dV < 0$ is can also be done. This is by using regulated reactive power compensation having sufficient control range and high Q/V gain with an opposite polarity [2].

The analysis we have presented in this section is limited to radial systems in order to make the understanding of different power system stability concepts much easy. But in complex power systems there are many factors that contribute to the system instability and can be studied at a higher level.

2.7 Some Significant Results and Criteria in Voltage Stability

In this section we present a summary of certain other significant criteria and results in voltage stability studies which have not been mentioned in the previous sections. These concepts have been mainly obtained from [4].

- Voltage stability limit is reached when $\left|\frac{S}{Y_{LL}^* V^2}\right| = 1$ [4]. (2.14)

  S is the complex power at load bus, Y_{LL} is the load bus admittance and V is the voltage at the load bus.

- The limit of maximum loading of a transmission line can be given by [4]

  $$|S| = V_{cri}^2 / X_{cri} \tag{2.15}$$

  Where X_{cri} is the critical reactance of the system after which voltage instability occurs. It is expressed as [4] $X_{cri} = \frac{E^2}{2P}(-\tan\phi + \sec\phi)$ (2.16)

- $\frac{dE}{dV}$ Criterion [4]. The voltage stability limit is reached when

  $$\cos\delta\left\{\frac{dQ}{dV} + \frac{2V}{X}\right\} + \sin\delta\frac{dP}{dV} - \frac{E}{X} = 0 \tag{2.17}$$

- $\frac{dZ}{dV}$ Criterion [4]. The value of critical impedance beyond which voltage instability occurs can found from this criteria. Voltage instability occurs when $\frac{dZ}{dV} = 0$

In this chapter we have tried to present a simple and clear understanding of the voltage stability concepts. An advanced level of analytical methods for voltage stability and rotor angle stability, which often go hand in hand, has been described in [2].

3. Power System Modeling and Thevenin Equivalent Circuit Parameters Estimation

In this Chapter, we will be estimating the Thevenin parameters for the power system model that has been built in MATLAB and SimPower system. The six bus power system model is represented in Figure 3.1[14]. The various SIMULINK blocks that have been used in the model have been studied in the initial sections of this Chapter. The block parameters have been represented in tables for each block. The power system model is simulated and the results are tabulated which are used for calculating the Thevenin parameters for the power system model built for this thesis research. The maximum power transferred is also calculated. The simulation results are also represented in terms of voltage and current signal waveforms at the end of this chapter.

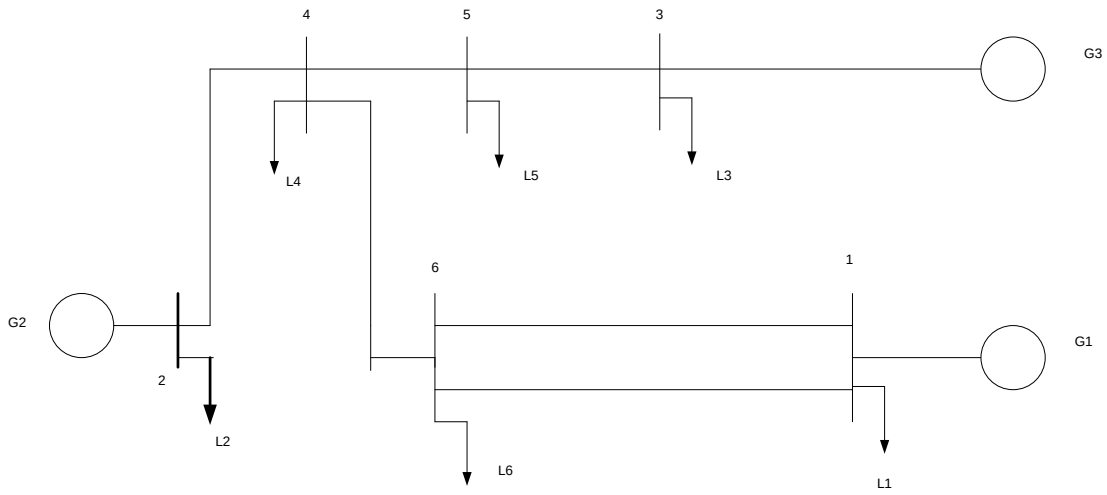

Figure 3.1 Six Bus Power System Model

3.1 Transmission Line Data

The transmission lines in the power system model have been represented by the three phase mutual inductance block in the SimPower system. It is to be noted that the block parameters in this SimPower system block are resistance and inductance whereas the data used has resistance and reactance values.

So, by using, $X = 2\pi fL$ (3.1)

For a system frequency of 60 Hz and individual reactance values as mentioned in the table, the corresponding inductance values have been calculated.

3.2 Generator Data

The generators have been represented by a three phase source block of SimPower system which is a three phase voltage source in series with RL branch. The block parameters of this block are:

(a) Phase-to-Phase rms voltage (V)
(b) Phase Angle of Phase A (degrees)
(c) Frequency (Hz)
(d) Source Resistance (Ohms) and Source Inductance (Henry)

The Values for the above parameters have been set as show in Table 3.1[10].

Table 3.1 Generators Block Parameter Values

Parameter	**Value**
Phase-to-Phase rms Voltage (v)	$\sqrt{3}$
Phase Angle of Phase A (degrees)	Varied from 0 to 60 for G2 ; 10 for G1 and 30 for G3
Frequency(Hz)	60
Source Resistance (Ohms) and Source Inductance (Henry)	0.001 (Ohms) and 0.001/377(Henry) Respectively.

The phase angle at Generator 2 is varied from 0 to 60 degrees and the three phase current and voltage waveforms have been plotted, which is shown later in this chapter.
The three voltage sources are connected in Wye with a neutral connection that has been internally grounded as obtained from [10].
The source impedance values of the generators are represented in the table 3.2. Equation 3.1 is used to convert the reactance values into the inductance and subsequently entered in the parameter block of the SimPower system model.

3.3 Load Data

A three-phase series RLC load block from the SimPower system has been used. RLC elements are combined in series to implement the three phase balanced load [10].
The parameters in this block have been set as shown in Table 3.2

Table 3.2 Load Block Parameter Values

Parameter	**Value**
Nominal Phase to Phase Voltage Vrms (V)	1
Nominal Frequency (Hz)	60
Active Power P (W)	0.25
Inductive Reactive Power(Var)	0.1
Capacitive Reactive Power(Var)	0

The configuration of the block is set to Wye (floating). Thus, the connection of the three phases is in Wye with neutral inaccessible.

3.4 Algorithm for Thevenin Equivalent Circuit Estimation

The six bus power system model in Figure 3.1 can be represented by its Thevenin equivalent circuit as referred from load bus L3 or L5 as shown in Figure 3.2.
The Thevenin equivalent parameters can be obtained by writing the network equations as seen from load bus L3 or L5.

$$E_S - Z_S I_K = V_k \tag{3.2}$$

Equation (3.2) represents the Network Equation for Figure 3.2.
E_S is the Source Voltage, Z_S is the Source Impedance.

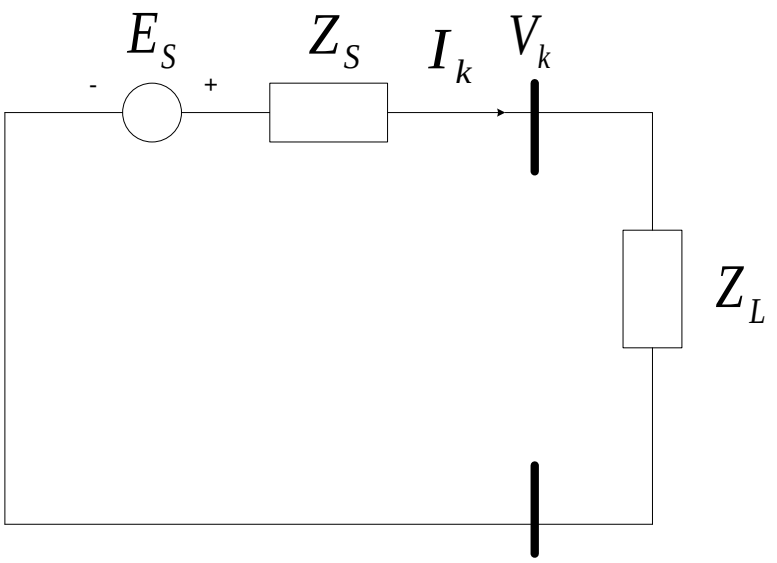

Figure 3.2 Thevenin Equivalent Circuit

At bus k, the Voltage and Current is represented by V_k and I_k respectively.

Equation (3.2) can be written for various values of currents and voltages at the bus k. This is done by varying the phase angle at one of the generators. In the power system model shown in Figure 3.1, the generator phase angles at G2 are varied first in order to get different values of currents and voltages at the bus k. So, Equation (3.2) can be further written as

$$E_S - Z_S I_{K1} = V_{k1} \tag{3.3}$$

$$E_S - Z_S I_{K2} = V_{k2} \tag{3.4}$$

For n values of generator angles, the Equation (3.2) can give n values of currents and voltages at the bus k.

Expressing it in the form $AX = B$,

$$\begin{bmatrix} 1 & -I_{k1} \\ 1 & -I_{k2} \\ . & . \\ . & . \\ 1 & -I_{kn} \end{bmatrix} \begin{bmatrix} E_s \\ Z_s \end{bmatrix} = \begin{bmatrix} V_{k1} \\ . \\ . \\ . \\ V_{kn} \end{bmatrix} \tag{3.5}$$

A is an $(nx2)$ Matrix.

X is a $(2x1)$ Matrix and B is an $nx1$ Matrix.

The solution for Equation (3.5) is obtained using the Least Mean Squares technique.

$$X = (A^T A)^{-1}(A^T B)$$

Thus the Thevenin equivalent parameters are calculated.

In the power system model represented in Figure 3.1, the phase angles at G2 are varied from 0 to 60 degrees to get the Thevenin equivalent voltage and current at the load, L3. The results are tabulated as shown in Table 3.3

Table 3.3 Voltage and Currents at Bus L3

Angle at Generator 2 (Degrees)	Voltage at bus 3 (p.u.) Magnitude(angle in degree)	Current at bus 3 (p.u.)	Active Power P (p.u.)	Reactive Power Q (p.u.)
0	1.252 (12.62)	0.97(12)	1.821	0.01968
10	1.257(13.11)	0.8362(13.5)	1.577	-0.00953
20	1.26(13.63)	0.7006(13.5)	1.324	0.001912
30	1.262(14.17)	0.567 (11.3)	1.072	0.05371
40	1.261 (14.72)	0.444 (4.8)	0.8271	0.1442
60	1.254 (15.75)	0.3082 (-32)	0.3894	0.4294

At load bus L5, the currents and voltages are tabulated by varying the phase angle of the generator G1. This is represented in Table 3.4

Table 3.4Voltage and Current at Load Bus L5

Angle at Generator 1 (Degrees)	Voltage at bus 5 (p.u.) Magnitude(angle in degree)	Current at bus 5 (p.u.)	Active Power P (p.u.)	Reactive Power Q (p.u.)
0	1.223(-5.411)	0.9163(2.452)	1.665	-0.2299
10	1.229(-1.684)	0.5881(3.134)	1.08	-0.09098
20	1.226(2.047)	0.267(-6.839)	0.4851	0.07585
30	1.1214(5.761)	0.1562(-105.2)	-0.1016	0.2655
40	1.194(9.441)	0.4544(-135.1)	-0.6624	0.4723
60	1.128(16.61)	1.109(-134.3)	-1.638	0.9116

Using these values of voltage and current at the buses, the Thevenin parameters have been calculated. The Thevenin parameters for different sets of measurements are tabulated in Tables 3.5 and 3.6

Table 3.5Thevenin Parameters for 4, 5 and 6 sets of measurements at Load bus L3

Number of Sets of Measurements	E_S		Z_S	
	E_{SR}	E_{SM}	R_S	X_S
4	1.2273	0.3586	0.0240	0.0846
5	1.227	0.3588	0.0237	0.0849
6	1.2270	0.3587	0.0236	0.0848

Table 3.6Thevenin Parameters for 4, 5 and 6 sets of measurements at Load bus L5

Number of Sets of Measurements	E_S		Z_S	
	E_{SR}	E_{SM}	R_S	X_S
4	1.1827	0.1078	-0.0483	0.2437
5	1.2170	0.109	0.0094	0.2483
6	1.2283	0.1059	0.0351	0.2463

E_S is the Source Voltage. Z_S is the Source Impedance.

E_{SR} and E_{SM} represent the Thevenin Voltage real and imaginary parts respectively.

R_S and X_S represent the Thevenin Resistance and Reactance respectively.

3.5 Equation for Maximum Power Delivered

From circuit theory, maximum power is delivered to a load when the source impedance value is equal to the load impedance [9].

$|Z_L| = |Z_S|$, where $|Z_L|$ is the impedance at the load and $|Z_S|$ is the source impedance.

Suppose load power factor angle is α. Then, $Z_L = |Z_L| \angle \alpha$.

From the Network in Figure 3.3[9], we can write $I = \dfrac{E_s}{Z_S + Z_L}$

The Power delivered is given by $S = P + jQ = (Z_L.I).I^*$

$$= Z_L |I|^2$$

$$= Z_L \left| \frac{E_s}{Z_s + Z_L} \right|^2$$

The power delivered at the load buses L3 and L5 for the system which we modeled is shown in Tables 3.7 and 3.8

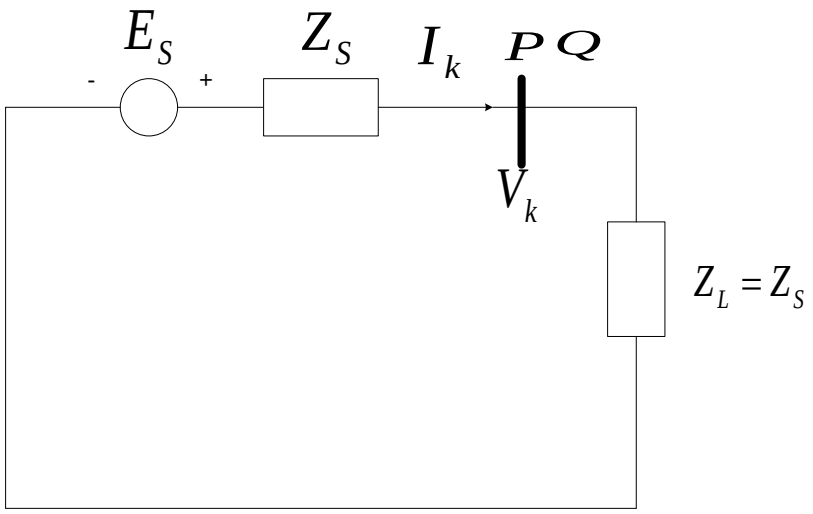

Figure 3.3 Equivalent Power System Model for Calculating Maximum Power Delivered

Table 3.7 Power Delivered at the Bus L3 for Different Power Factor angles

Angle	P (p.u)	Q (p.u)
0	7.3202	-
10	6.3869	1.1262
20	5.5158	2.0076
30	4.6906	2.7081
40	3.8972	3.2702

Table 3.8 Power Delivered at the Bus L5 for Different Power Factor angles

Angle	P (p.u)	Q (p.u)
0	2.6770	
10	2.2949	0.4047
20	1.9511	0.7102
30	1.6358	0.9444
40	1.3414	1.1256

3.6 Voltage and Current Waveforms at Load Bus L3

The voltage and current waveforms are plotted by varying the phase angles at G2 and G3. This is represented in the figures in this section

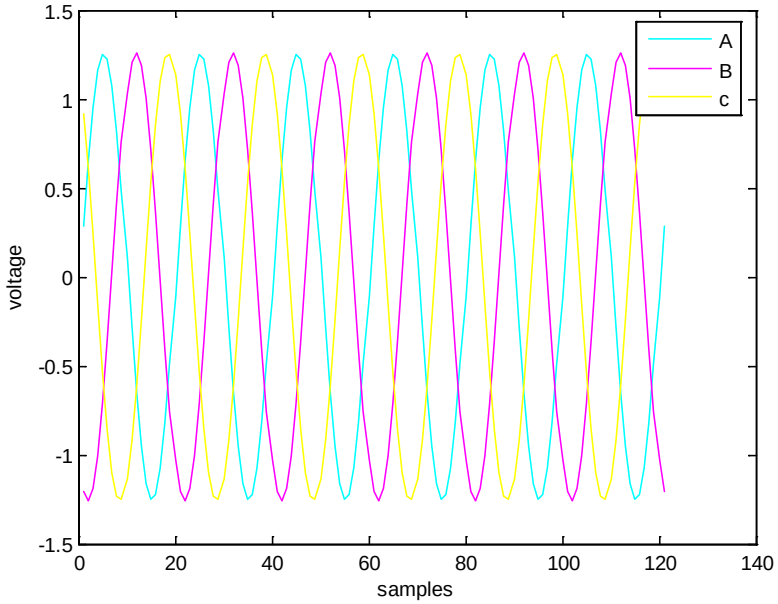

Figure 3.4(a) Voltage signals for the case with generator 2 angles set to 10 degrees.

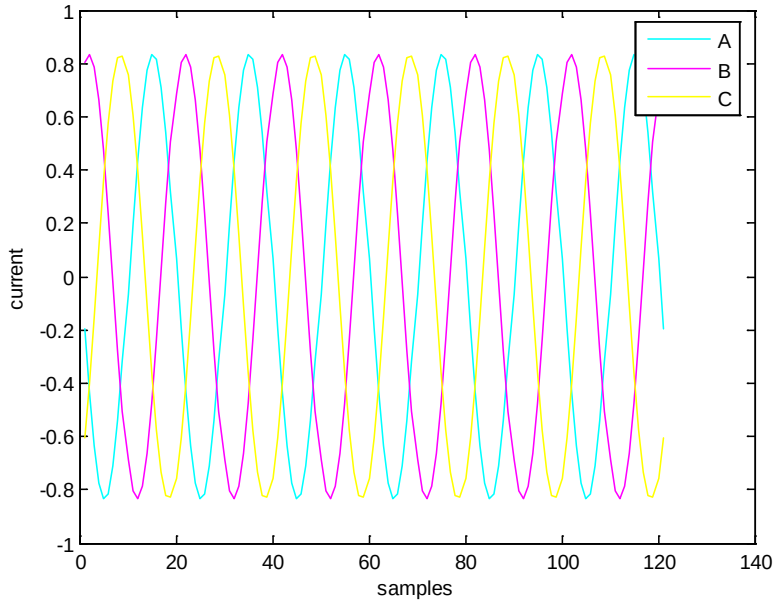

Figure 3.4(b) Current signals for the case with generator 2 angles set to 10 degrees.

.

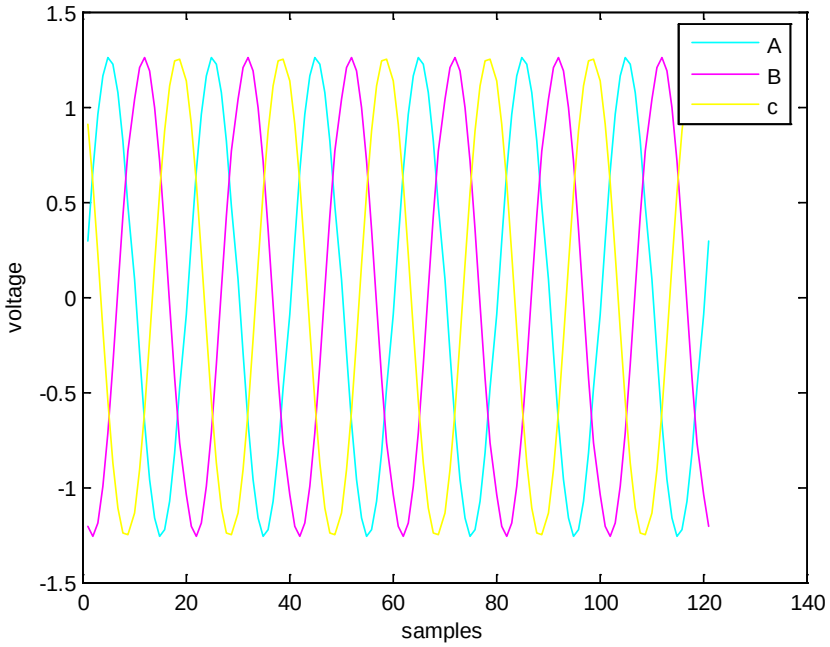

Figure 3.5(a) Voltage signals for the case with generator 2 angles set to 20 degrees

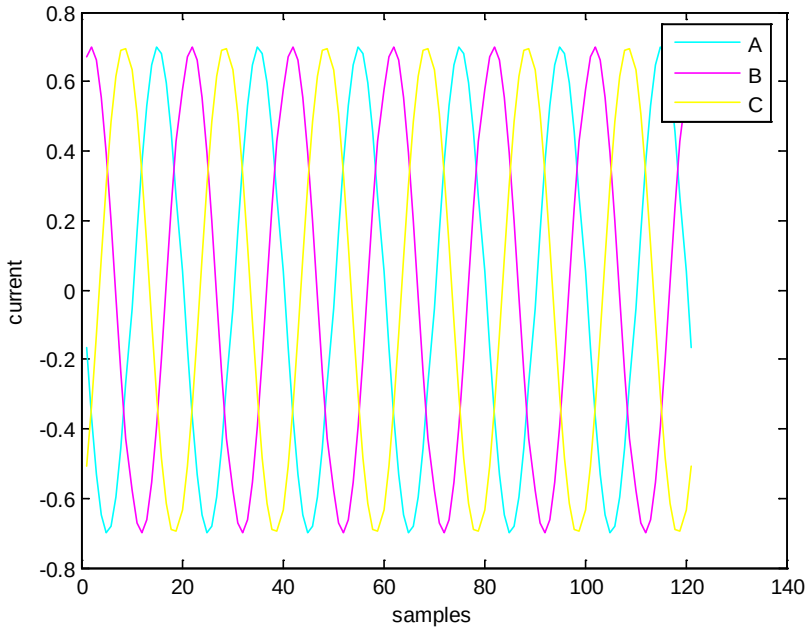

Figure 3.5(b) Current signals for the case with generator 2 angles set to 20 degrees

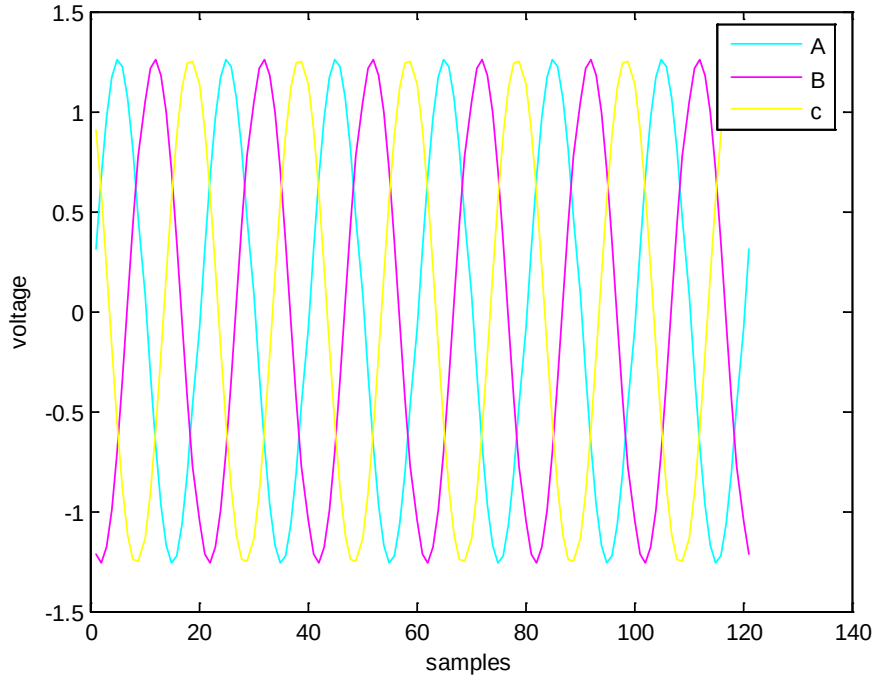

Figure 3.6(a) Voltage signals for the case with generator 2 angles set to 30 degrees

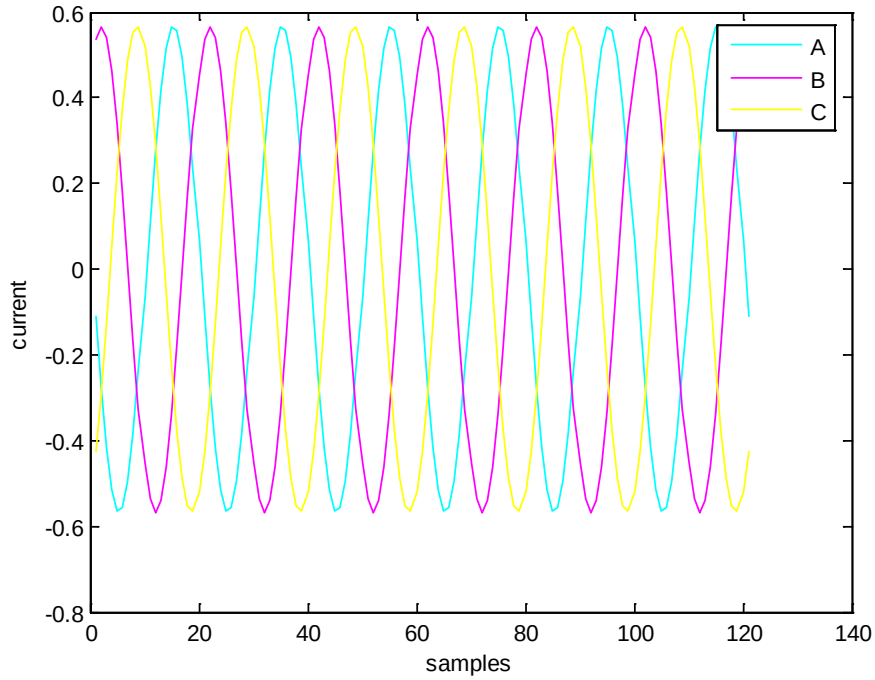

Figure 3.6(b) Current signals for the case with generator 2 angles set to 30 degrees

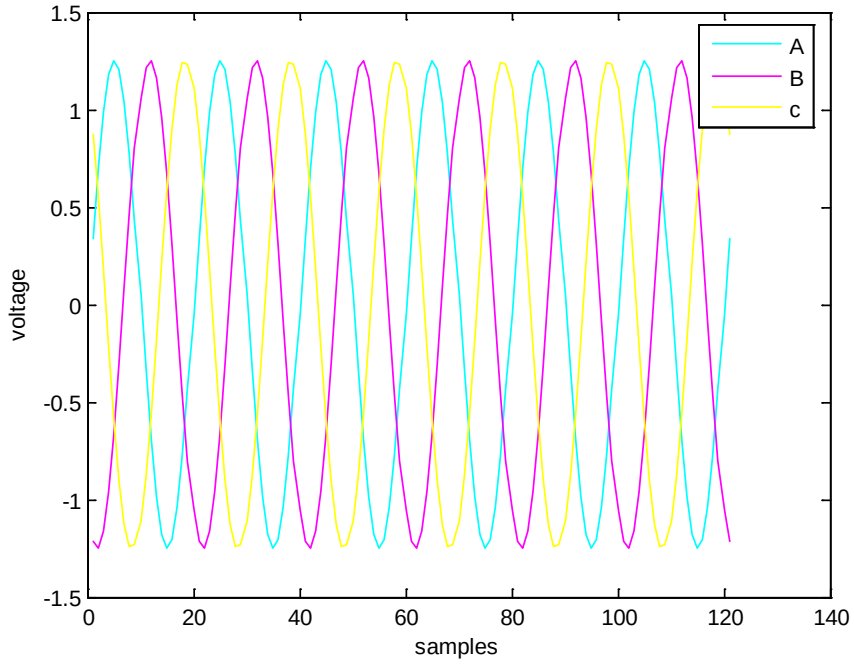

Figure 3.7(a) Voltage signals for the case with generator 2 angles set to 40 degrees

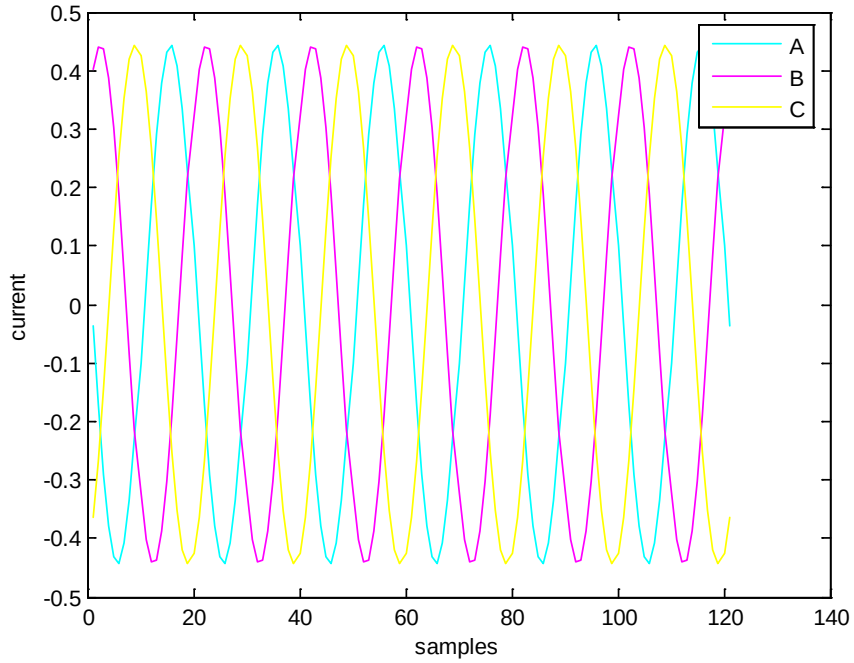

Figure 3.7(b) Current signals for the case with generator 2 angles set to 40 degrees

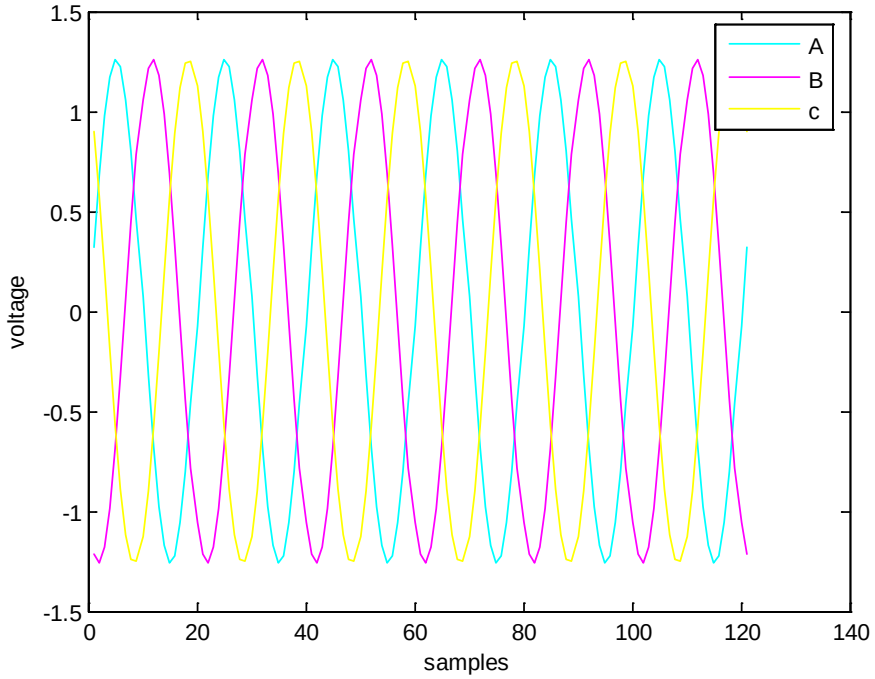

Figure 3.8(a) Voltage signals for the case with generator 2 angles set to 60 degrees

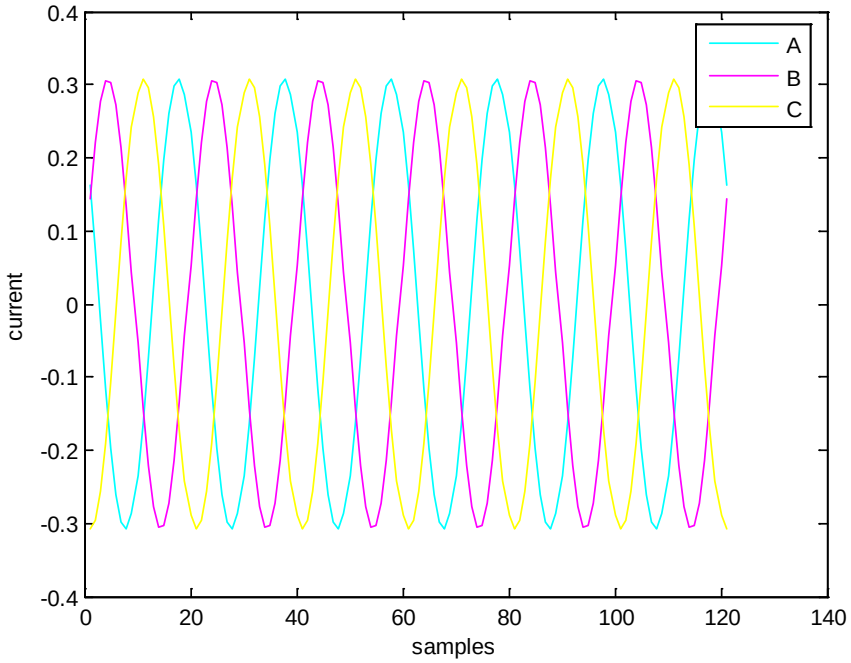

Figure 3.8(b) Current signals for the case with generator 2 angles set to 60 degrees

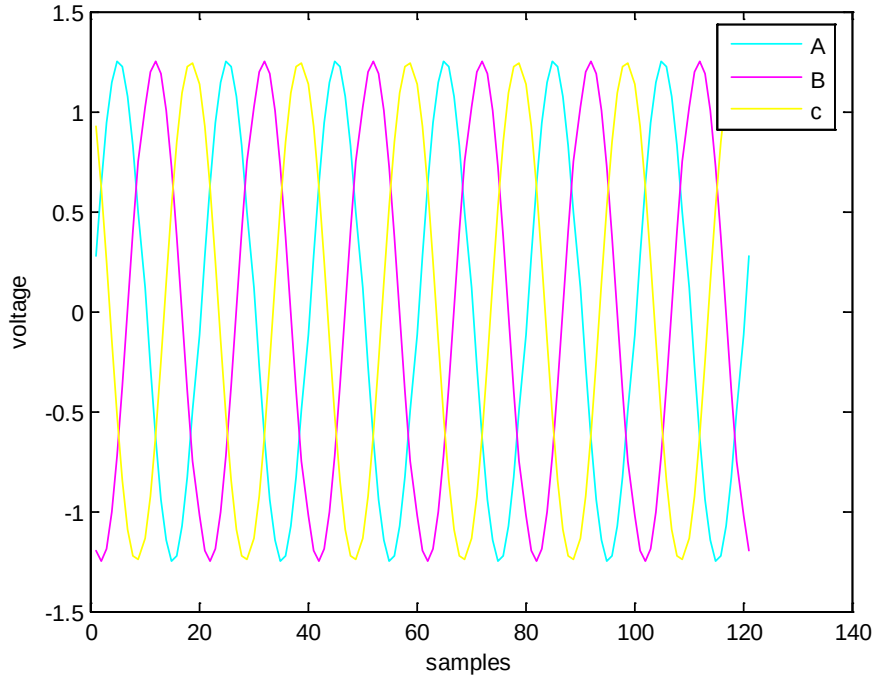

Figure 3.9(a) Voltage signals for the case with generator 2 angles set to 0 degrees

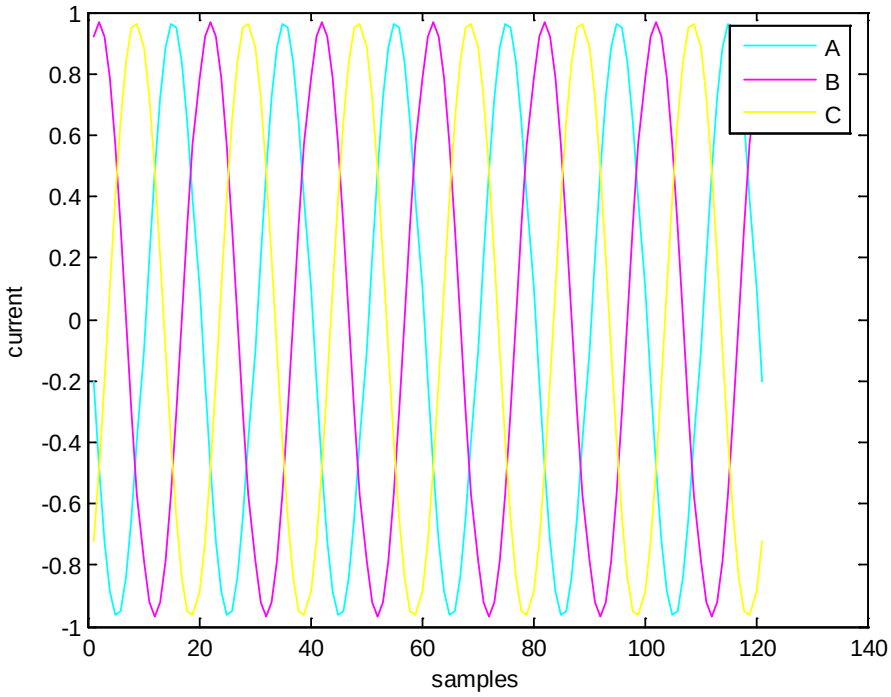

Figure 3.9(b) Current signals for the case with generator 2 angles set to 0 degrees

3.7 Waveforms for Voltage and Current at the Load bus L5

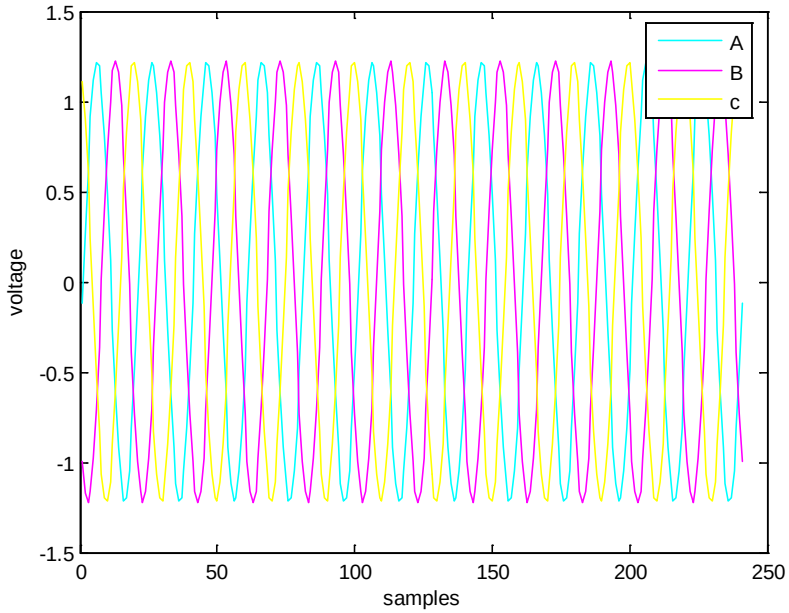

Figure 3.10(a) Voltage signals for the case with generator 3 angles set to 0 degrees

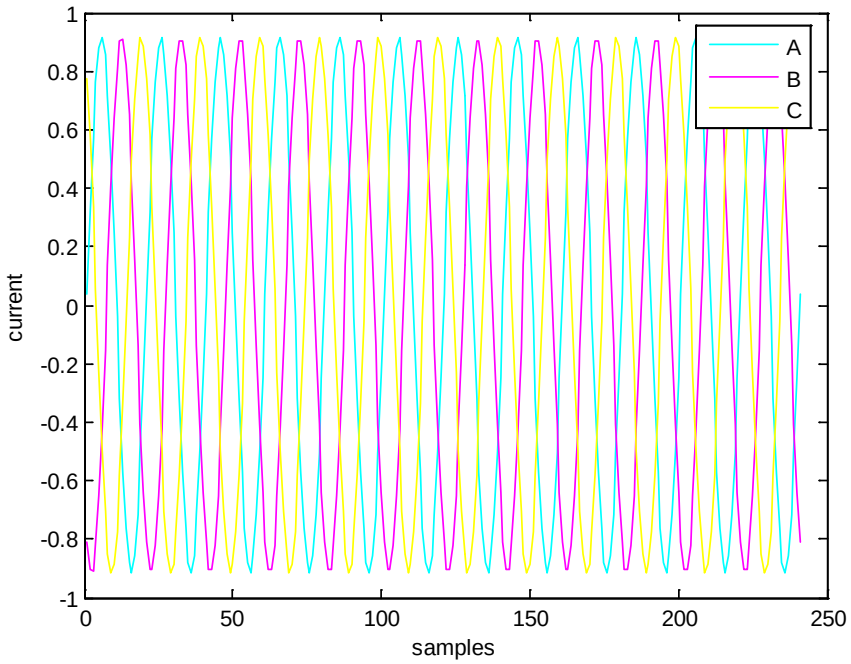

Figure 3.10(b) Current signals for the case with generator 3 angles set to 0 degrees

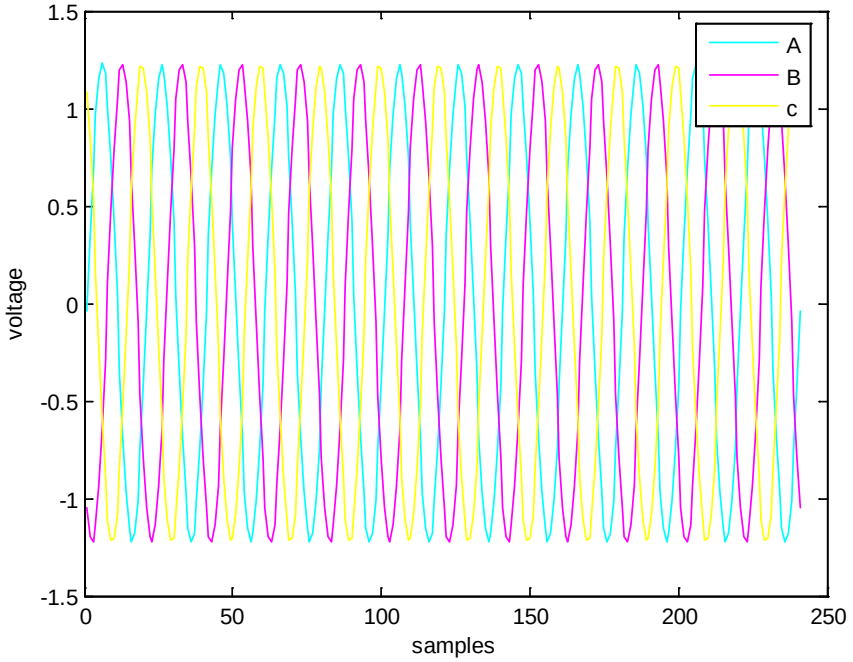

Figure 3.11(a) Voltage signals for the case with generator 3 angles set to 10 degrees

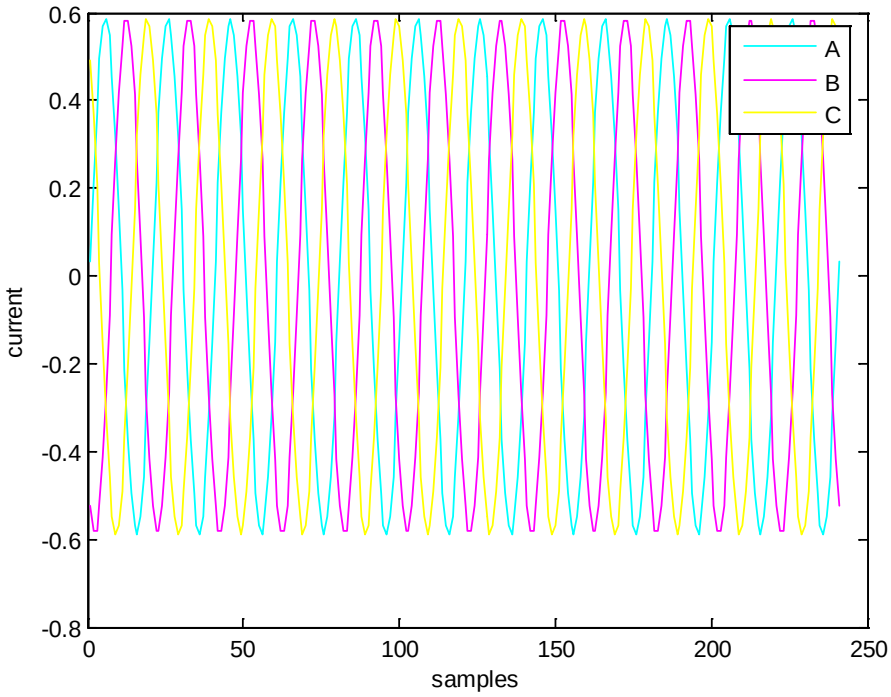

Figure 3.11(b) Current signals for the case with generator 3 angles set to 10 degrees

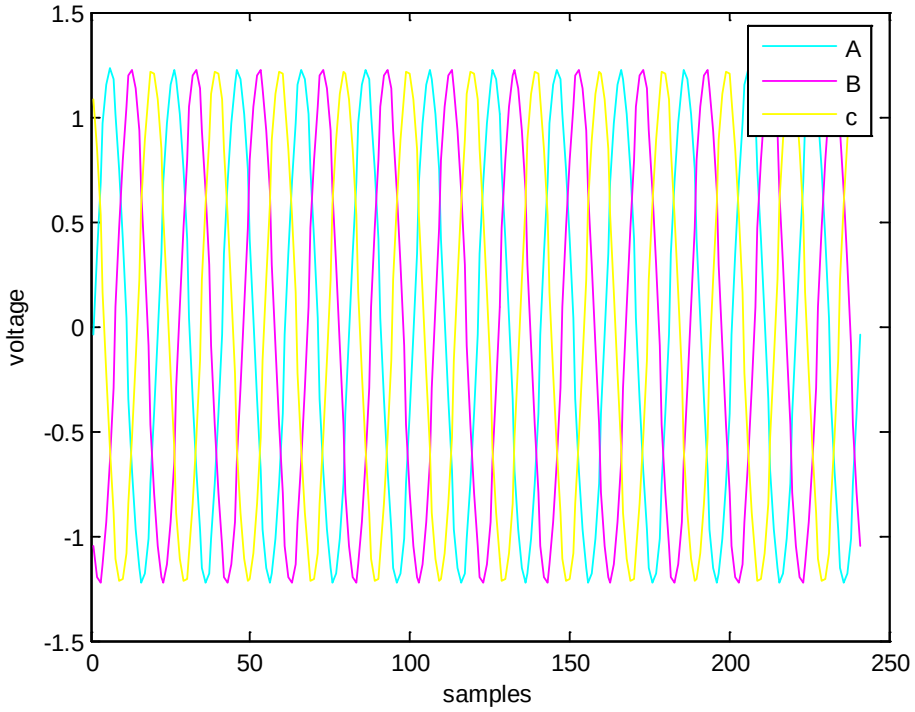

Figure 3.12(a) Voltage signals for the case with generator 3 angles set to 20 degrees

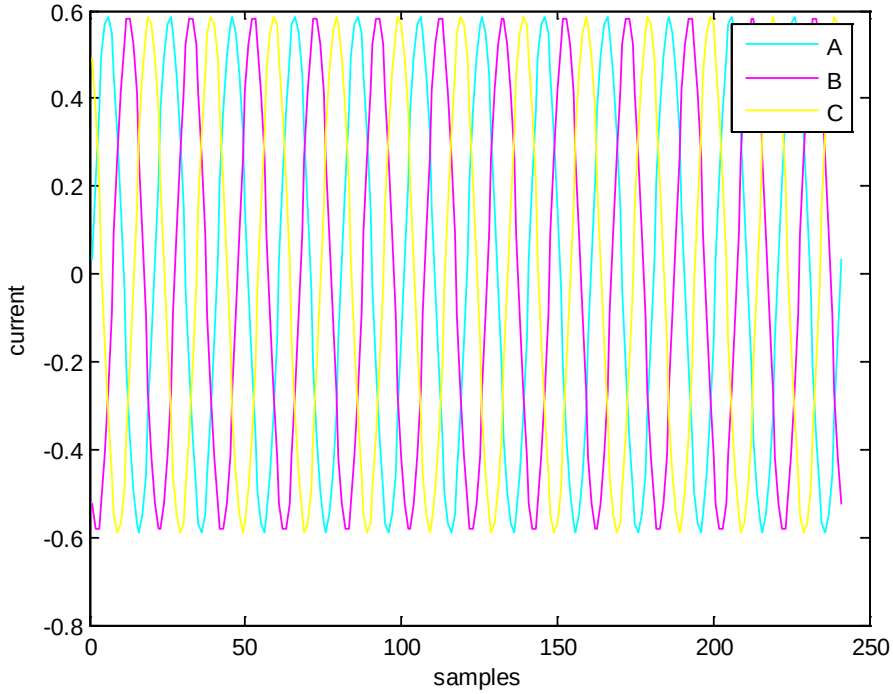

Figure 3.12(b) Current signals for the case with generator 3 angles set to 20 degrees

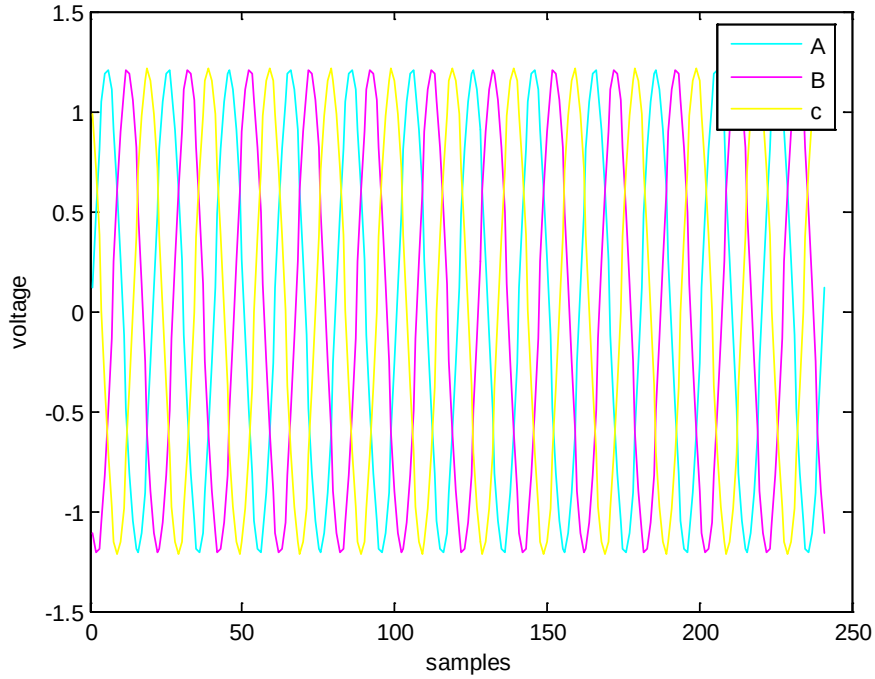

Figure 3.13(a) Voltage signals for the case with generator 3 angles set to 30 degrees

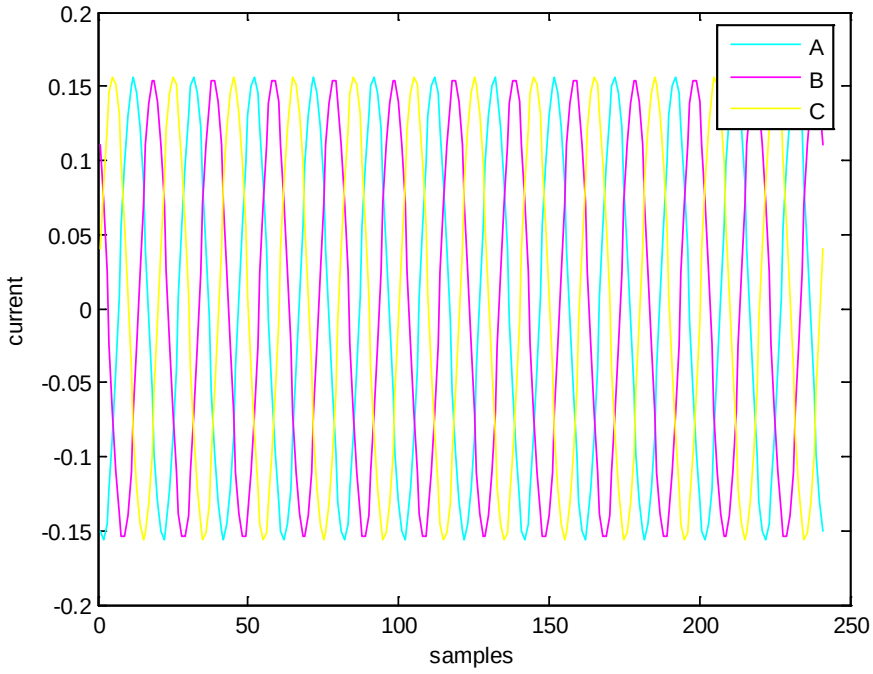

Figure 3.13(b) Current signals for the case with generator 3 angles set to 30 degrees

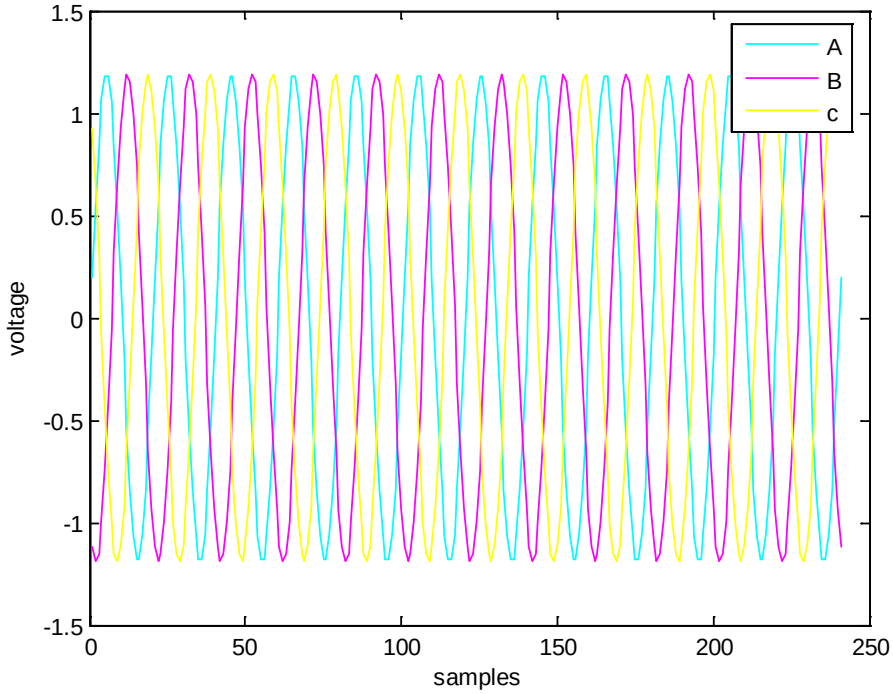

Figure 3.14(a) Voltage signals for the case with generator 3 angles set to 40 degrees

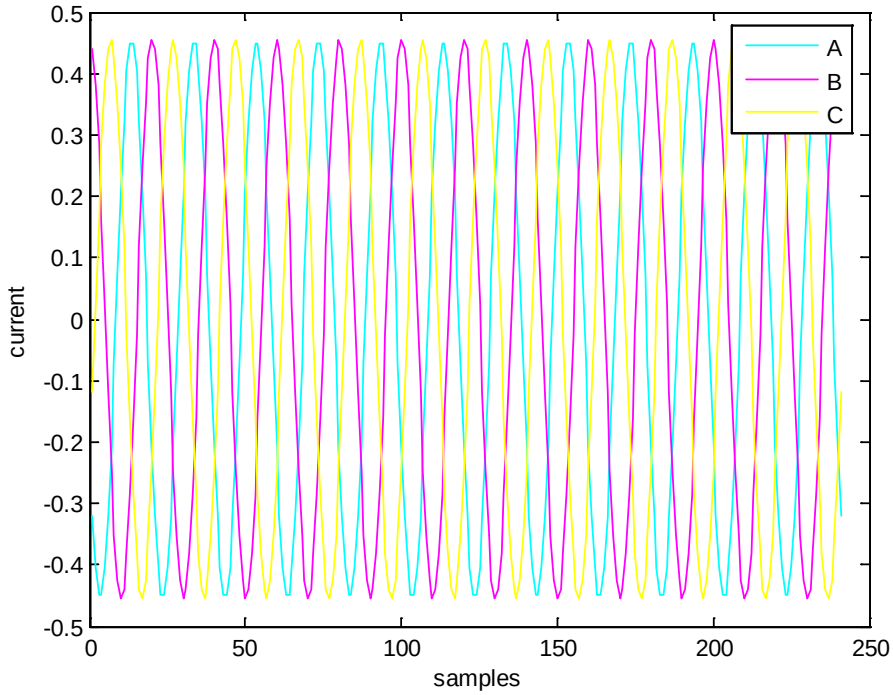

Figure 3.14(b) Current signals for the case with generator 3 angles set to 40 degrees

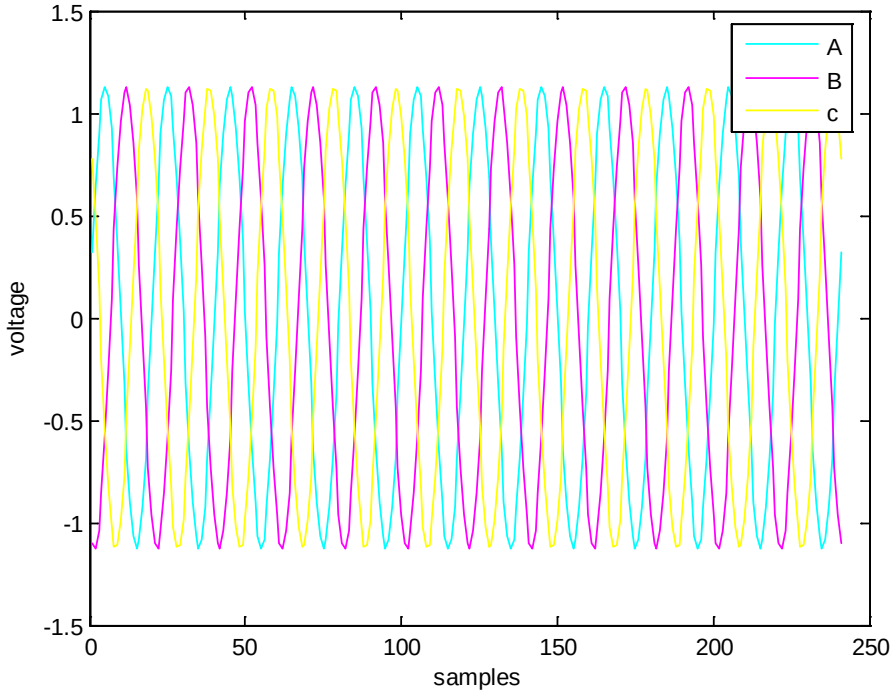

Figure 3.15(a) Voltage signals for the case with generator 3 angles set to 60 degrees

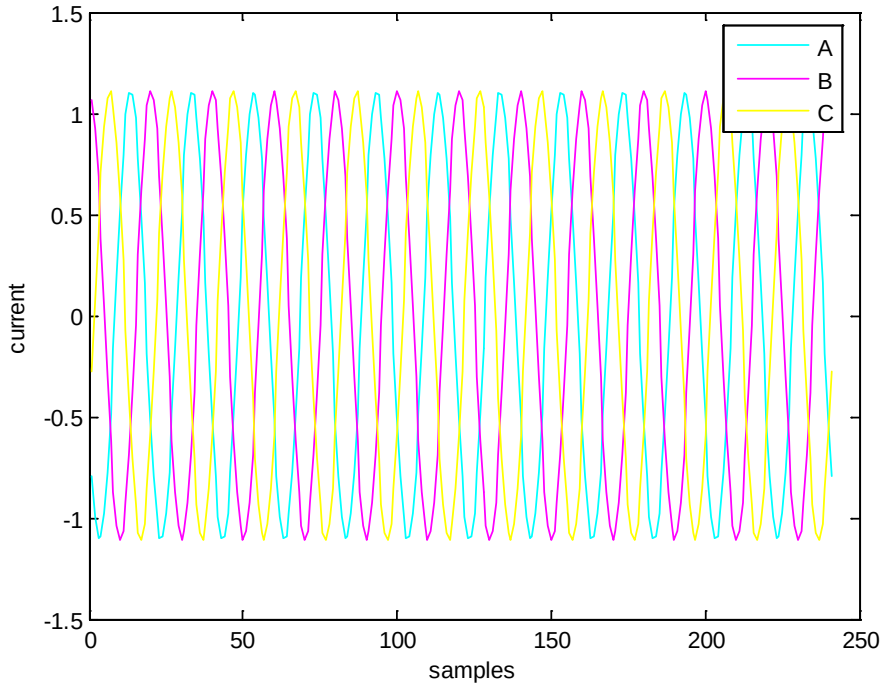

Figure 3.15(b) Current signals for the case with generator 3 angles set to 60 degrees

4. Fault Analysis and Estimation of Fault Location

In this Chapter, we will be studying the concepts of unsymmetrical fault analysis and also the algorithms that have been proposed in Dr. Liao's work, "Fault location utilizing unsynchronized voltage measurements during fault", *Electric Power Components & Systems*, vol. 34, no. 12, December 2006, pp. 1283 – 1293. One of the algorithms has been used to estimate the fault location for my power system model. The shunt capacitances have been neglected in the algorithm used for estimation in order to have simplicity and computational efficiency. The Thevenin parameter values obtained for the power system model of Chapter 3 have been used in the fault location algorithm in [5] to calculate the fault location for the model used in this thesis. The current and voltage signal waveforms for the different values of fault location have been presented at the end of this chapter.

In the initial sections of this chapter, the basic concepts of unsymmetrical fault analysis have been presented. The equations and figures of unsymmetrical fault analysis in sections (4.1-4.5) have all been obtained from [4] and we explain it as much as possible.

4.1 Unsymmetrical Faults

The unsymmetrical faults can be classified as shunt type faults and series type faults.
Shunt type faults can again be classified as [4]:

(a) Single Line to Ground fault
(b) Line to Line Fault
(c) Double Line to Ground fault

Before we study in detail about the shunt type faults, it is important to study the symmetrical component analysis of unsymmetrical faults.

4.2 Symmetrical Component Analysis of Unsymmetrical Faults

In this section, we will analyze how a power network which is under a fault condition can be represented in terms of positive, negative and zero sequence networks as seen from the point where the fault is occurring.

Figure 4.1 represents a general power network [4]. F is the point of fault occurrence. When the fault occurs in the system, the currents are represented by I_a, I_b, I_c as shown, which flow out of the system. The voltages of lines a, b, c with respect to the ground are V_a, V_b, V_c respectively.

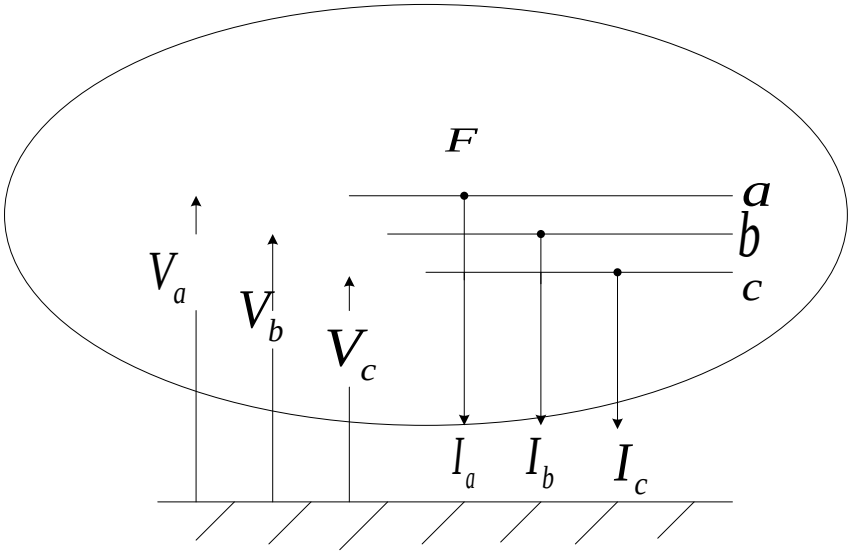

Figure 4.1 A General Power Network

Before the fault occurs, the positive sequence voltages of all synchronous machines in the network are given by E_a. This is the pre fault voltage at F.

The positive, negative and zero sequence networks after the occurrence of the fault as seen from F are represented in Figures 4.2 (a), (b) and (c) [4].

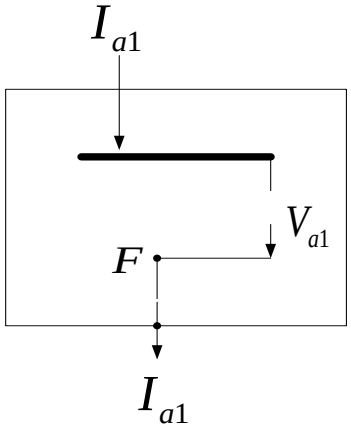

Figure 4.2 (a) Positive sequence network as seen from the fault point

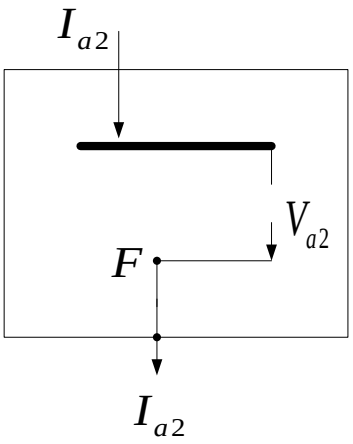

Figure 4.2 (b) Negative Sequence Network as seen from the fault point

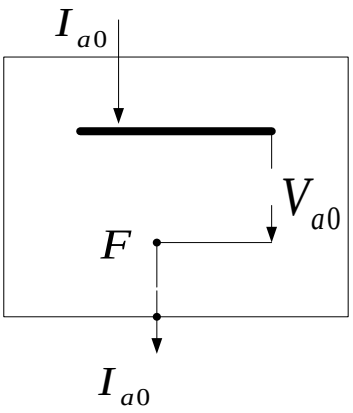

Figure 4.2(c) Zero sequence Network as seen from the fault point

The Thevenin equivalents of the sequence networks are represented in Figure 4.2 (d), (e), (f) [4]

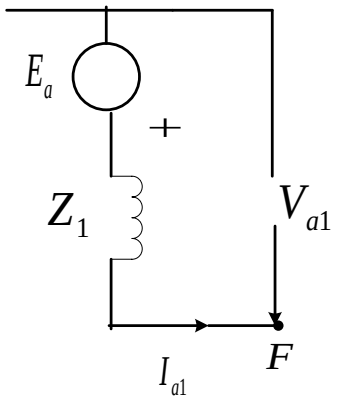

Figure 4.2 (d) Thevenin Equivalent of Positive sequence Network as seen from F

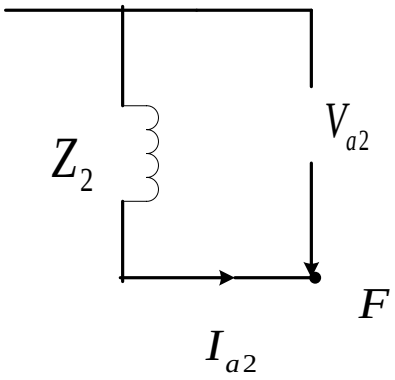

Figure 4.2 (e) Thevenin Equivalent of Negative sequence Network as seen from F

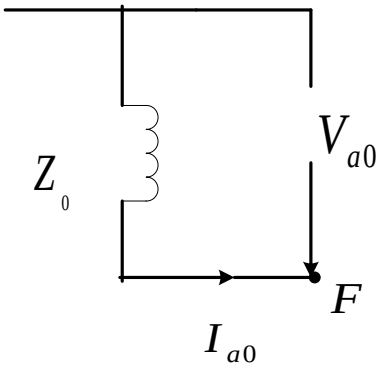

Figure 4.2 (f) Thevenin Equivalent of Zero sequence Network as seen from F

We have mentioned, E_a is present only in the positive sequence network. We can express the sequence voltages at F as shown in Equation (4.1) [4].

$$\begin{bmatrix} V_{a1} \\ V_{a2} \\ V_{a0} \end{bmatrix} = \begin{bmatrix} E_a \\ 0 \\ 0 \end{bmatrix} - \begin{bmatrix} Z_1 & 0 & 0 \\ 0 & Z_2 & 0 \\ 0 & 0 & Z_0 \end{bmatrix} \begin{bmatrix} I_{a1} \\ I_{a2} \\ I_{a0} \end{bmatrix} \tag{4.1}$$

V_{a1}, V_{a2}, V_{a0} are the Positive, negative and Zero Sequence Voltages respectively.

I_{a1}, I_{a2}, I_{a0} are the Positive, negative and Zero sequence Currents respectively.

Z_1, Z_2, Z_0 are the Positive, negative and Zero sequence Impedances respectively.

Now, we can analyze the different types of shunt faults based on the concepts presented in section 4.2. The expressions for fault currents and voltages in the lines are derived subsequently.

4.3 Analysis of Single Line to Ground Fault

Figure 4.3(a) shows the power network when a single line to ground fault occurs at point F [4]. The fault occurs on Phase a.

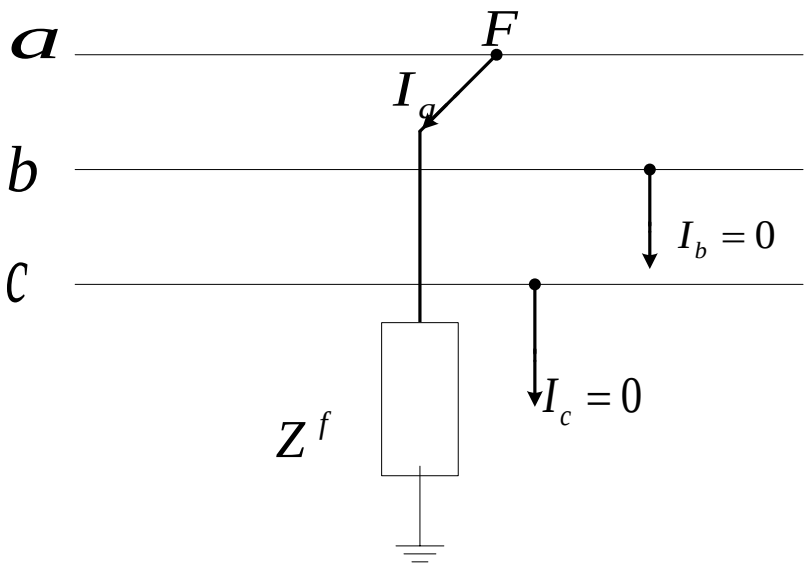

Figure 4.3(a) Single Line to Ground Fault at F

The equations for currents and the line to ground voltages are represented as follows [4]:

$$I_b = 0 \tag{4.2}$$

$$I_c = 0 \tag{4.3}$$

$$V_a = Z^f I_a \tag{4.4}$$

Using the symmetrical components method, we get the fault currents expressed in terms of positive, negative and zero sequence components as shown in Equation (4.5)[4].

$$\begin{bmatrix} I_{a1} \\ I_{a2} \\ I_{a0} \end{bmatrix} = \frac{1}{3}\begin{bmatrix} 1 & \alpha & \alpha^2 \\ 1 & \alpha^2 & \alpha \\ 1 & 1 & 1 \end{bmatrix}\begin{bmatrix} I_a \\ 0 \\ 0 \end{bmatrix} \tag{4.5}$$

Therefore,

$$I_{a1} = I_{a2} = I_{a0} = \frac{1}{3} I_a \tag{4.6}$$

From Eq. (4.4) and (4.6), we get

$$Z^f I_a = 3Z^f I_{a1} = V_{a1} + V_{a2} + V_{a0} \tag{4.7}$$

From the Equations (4.6) and (4.7), it can be analyzed that there is a series connection of sequence networks represented by Figure 4.3(b) [4].

The sequence components of fault current I_a and the voltages V_b and V_c can be found by using the Thevenin equivalents of the sequence networks which is shown in Figure 4.3(b). These are represented in Equation (4.8)-Equation (4.15)[4].

$$I_{a1} = \frac{E_a}{(Z_1 + Z_2 + Z_0) + 3Z^f} \tag{4.8}$$

The fault current I_a can thus be given by

$$I_a = 3I_{a1} = \frac{3E_a}{(Z_1 + Z_2 + Z_0) + 3Z^f} \tag{4.9}$$

Also by Using Eq. (4.1), the fault current I_a can be obtained.

$$(E_a - I_{a1}Z_1) + (-I_{a2}Z_2) + (-I_{a0}Z_0) = 3Z^f I_{a1} \tag{4.10}$$

$$\Rightarrow [(Z_1 + Z_2 + Z_0) + 3Z^f]I_{a1} = E_a \tag{4.11}$$

$$\Rightarrow I_{a1} = \frac{E_a}{(Z_1 + Z_2 + Z_0) + 3Z^f} \tag{4.12}$$

Now, making use of the method of symmetrical components and finding the voltage of line b to ground under fault conditions.

$$\Rightarrow V_b = \alpha^2 V_{a1} + \alpha V_{a2} + V_{a0} \tag{4.13}$$

Using the values of V_{a1}, V_{a2}, V_{a0} from Eq. (4.1) in (4.13), we get

$$V_b = \alpha^2\left(E_a - Z_1\frac{I_a}{3}\right) + \alpha\left(-Z_2\frac{I_a}{3}\right) + \left(-Z_0\frac{I_a}{3}\right) \tag{4.14}$$

Using Equation (4.9) in Equation (4.14)

$$V_b = E_a\frac{3\alpha^2 Z^f + Z_2(\alpha^2 - \alpha) + Z_0(\alpha^2 - 1)}{(Z_1 + Z_2 + Z_0) + 3Z^f} \tag{4.15}$$

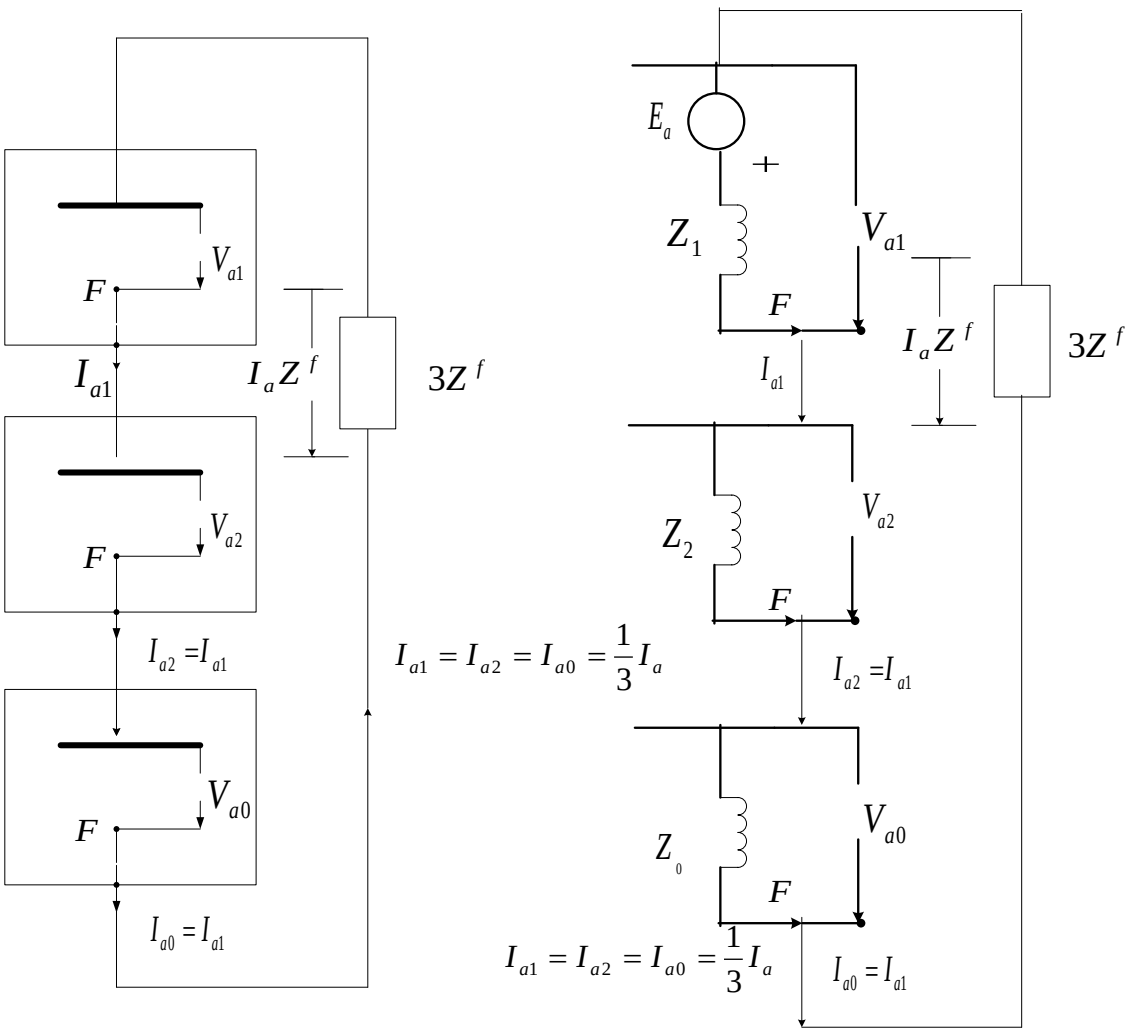

Figure 4.3(b) Connection of sequence networks for single Line to Ground Fault

4.4 Analysis of Line to Line Fault

In the Figure 4.4 a line to line fault through fault impedance Z^f is indicated as shown. The figures and equations in this section have all been obtained from [4].

The currents are expressed as [4]

$$I_a = 0 \tag{4.16}$$

$$I_b + I_c = 0 \tag{4.17}$$

$$\Rightarrow I_c = -I_b \tag{4.18}$$

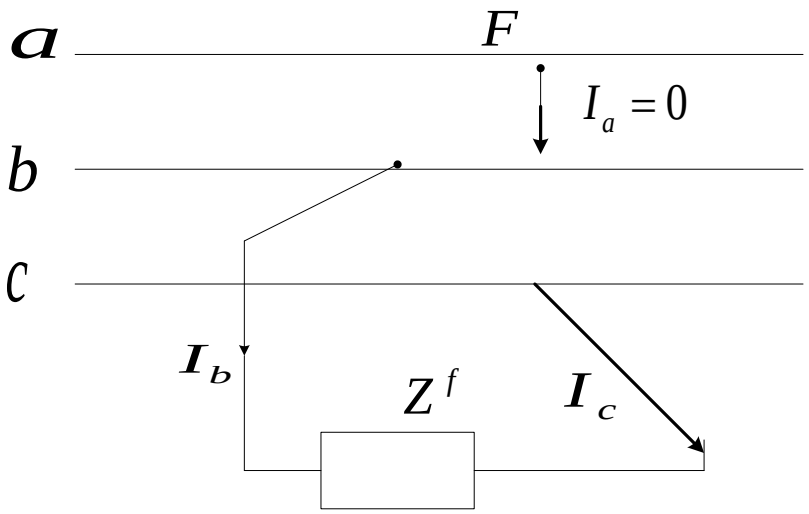

Figure 4.4(a) Line to Line Fault through Impedance Z^f

The voltage relationship between V_b and V_c is expressed as [4]

$$V_b - V_c = I_b Z^f \tag{4.19}$$

The positive, negative and zero sequence components of the fault currents are expressed as [4]

$$\begin{bmatrix} I_{a1} \\ I_{a2} \\ I_{a0} \end{bmatrix} = \frac{1}{3}\begin{bmatrix} 1 & \alpha & \alpha^2 \\ 1 & \alpha^2 & \alpha \\ 1 & 1 & 1 \end{bmatrix}\begin{bmatrix} 0 \\ I_b \\ -I_b \end{bmatrix} \tag{4.20}$$

On solving Equation (4.20), we get

$$I_{a2} = -I_{a1} \tag{4.21}$$

$$I_{a0} = 0 \tag{4.22}$$

Now, the symmetrical components of voltages under fault at F are expressed as [4]

$$\begin{bmatrix} V_{a1} \\ V_{a2} \\ V_{a0} \end{bmatrix} = \frac{1}{3}\begin{bmatrix} 1 & \alpha & \alpha^2 \\ 1 & \alpha^2 & \alpha \\ 1 & 1 & 1 \end{bmatrix}\begin{bmatrix} V_a \\ V_b \\ V_b - Z^f I_b \end{bmatrix} \tag{4.23}$$

From the Equation (4.23) expressing V_{a1} and V_{a2}

$$3V_{a1} = V_a + (\alpha^2 + \alpha)V_b - \alpha^2 Z^f I_b \tag{4.24}$$

$$3V_{a2} = V_a + (\alpha^2 + \alpha)V_b - \alpha Z^f I_b \tag{4.25}$$

Solving Equation (4.24) and (4.25)

$$3(V_{a1} - V_{a2}) = (\alpha - \alpha^2)Z^f I_b = j\sqrt{3}Z^f I_b \quad (4.26)$$

Using Equations (4.21) and (4.22) in (4.20)

$$I_b = (\alpha^2 - \alpha)I_{a1} = -j\sqrt{3}I_{a1} \quad (4.27)$$

Substituting Equation (4.27) in Equation (4.26)

$$V_{a1} - V_{a2} = Z^f I_{a1} \quad (4.28)$$

From Equations (4.21) and (4.28), we can draw a parallel connection of positive and negative sequence networks through Z^f as series impedance as shown in Figure 4.4(b)[4]. The zero sequence network is not connected as $I_{a0} = 0$. Its Thevenin equivalent is also represented in 4.4 (c)[4].

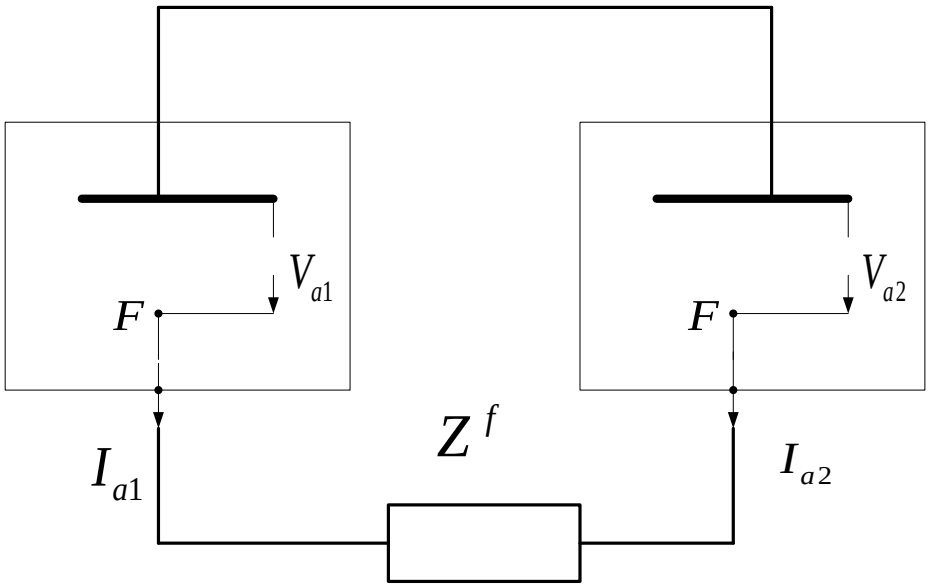

Figure 4.4(b) Positive and Negative Sequence Connections for a Line to Line Fault

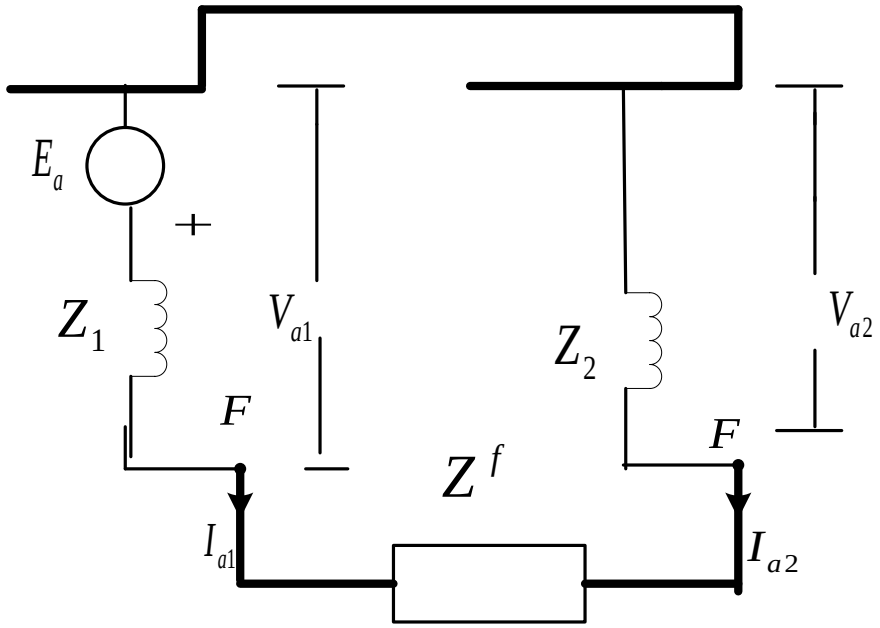

Figure 4.4(c) Thevenin Equivalent for connection of Sequence Networks for L-L Fault

By using the Thevenin equivalent, we can write the expressions for

$$I_{a1} = \frac{E_a}{Z_1 + Z_2 + Z^f} \tag{4.29}$$

$$I_b = -I_c = \frac{-j\sqrt{3E_a}}{Z_1 + Z_2 + Z^f} \tag{4.30}$$

The voltages at fault can be found out by knowing V_{a1} and V_{a2}. This can be calculated from I_{a1}.

4.5 Double Line to Ground Fault Analysis

In this section, we will make the analysis of a double line to ground fault. The figures and equations have all been obtained from [4].Figure 4.5(a) shows the double line to ground fault in a power system at a point F [4].

The fault current for a double line to ground fault is expressed as [4]

$$I_a = 0 \Rightarrow I_{a1} + I_{a2} + I_{a0} = 0 \tag{4.31}$$

The voltage to ground at fault conditions are expressed as [4]

$$V_b = V_c = Z^f (I_b + I_c) = 3Z^f I_{a0} \tag{4.32}$$

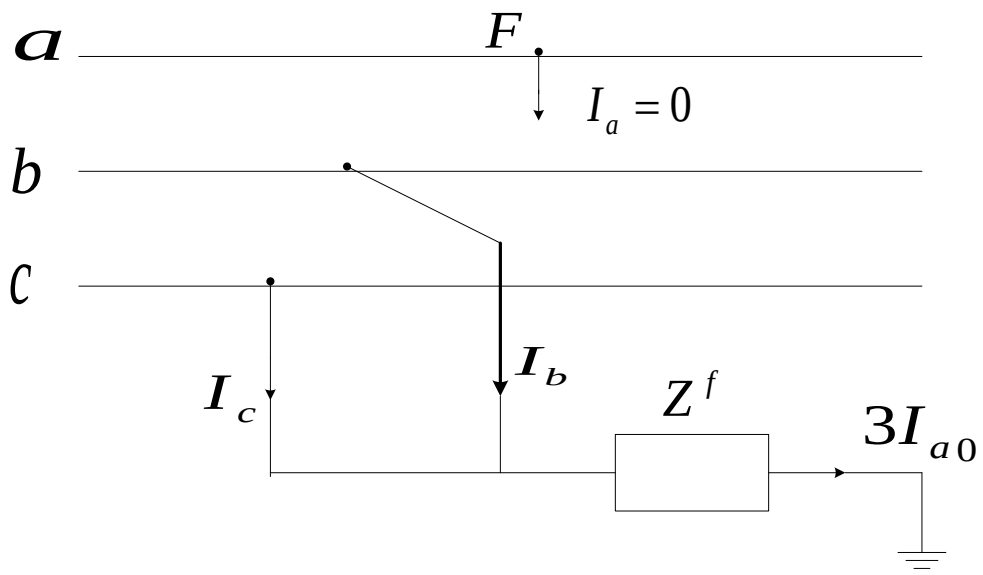

Figure 4.5(a) Double Line to Ground Fault through Impedance Z^f

The symmetrical components of voltages under fault at F are expressed as [4]

$$\begin{bmatrix} V_{a1} \\ V_{a2} \\ V_{a0} \end{bmatrix} = \frac{1}{3}\begin{bmatrix} 1 & \alpha & \alpha^2 \\ 1 & \alpha^2 & \alpha \\ 1 & 1 & 1 \end{bmatrix}\begin{bmatrix} V_a \\ V_b \\ V_b \end{bmatrix} \tag{4.33}$$

Thus,

$$V_{a1} = V_{a2} = \frac{1}{3}\left[V_a + (\alpha + \alpha^2)V_b\right] \tag{4.34}$$

$$V_{a0} = \frac{1}{3}(V_a + 2V_b) \tag{4.35}$$

From Equations (4.34) and (4.35)

$$V_{a0} - V_{a1} = \frac{1}{3}(2 - \alpha - \alpha^2)V_b = V_b = 3Z^f I_{a0} \quad [4] \tag{4.36}$$

$$\Rightarrow V_{a0} = V_{a1} + 3Z^f I_{a0} \tag{4.37}$$

Thus, the connection for the positive, negative and zero sequence networks can be drawn based on the equations obtained in this section.

Figure 4.5(b) represents the connection of sequence networks for a double line to ground fault [4].

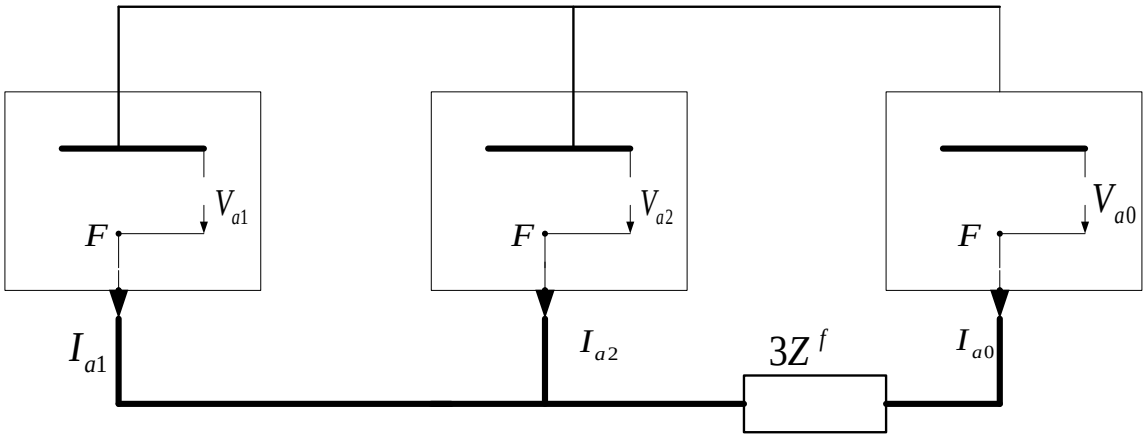

Figure 4.5(b) connection of sequence networks for a double line to ground fault

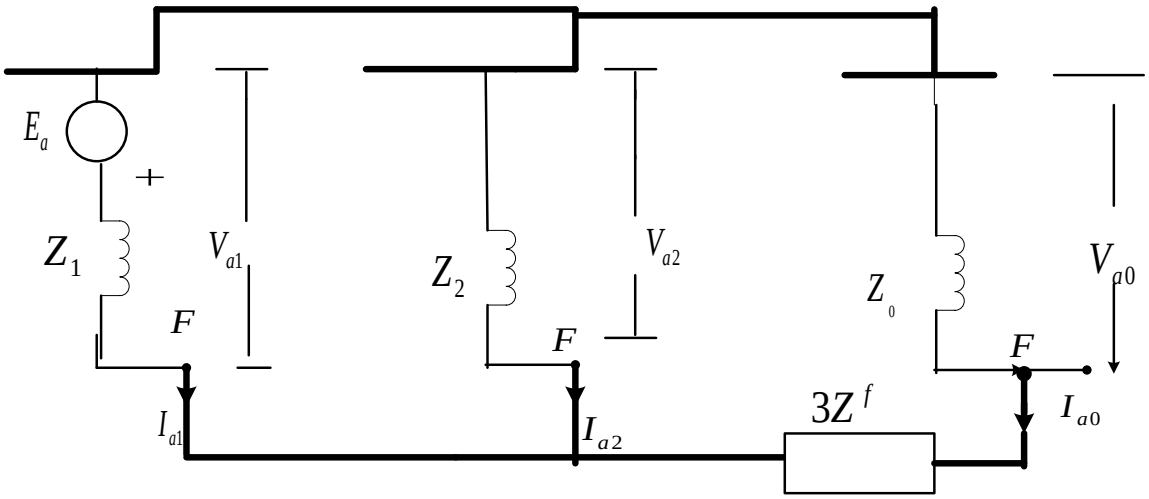

Figure 4.5(c) Thevenin Equivalent for the sequence network connections for a LLG fault

From Figure 4.5 (c) the following expressions can be written [4]

$$\Rightarrow I_{a1} = \frac{E_a}{Z_1 + Z_2(Z_0 + 3Z_f)/(Z_2 + Z_0 + 3Z^f)} \tag{4.38}$$

4.6 Fault Location Algorithm

In this section we study a fault location algorithm that has been presented in [5]. The impedance based algorithm is studied and made use in order to calculate the fault location. This algorithm is applicable for all kind of unsymmetrical faults [5]. For studying the algorithm we consider the transmission line represented in Figure 4.6.

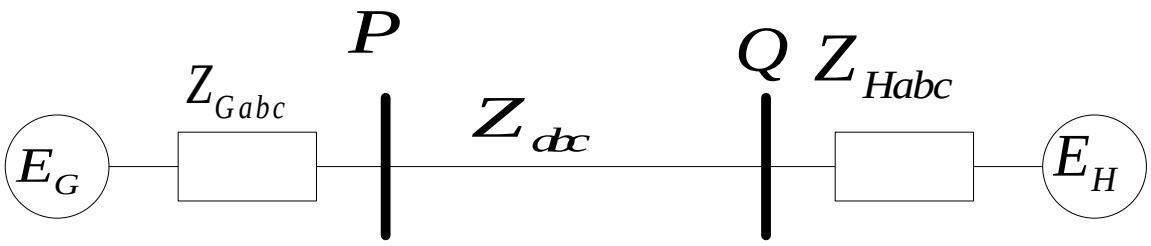

Figure 4.6 Transmission Line Considered for the Algorithm [5]

4.7 Impedance Based Algorithm

E_G, Z_{Gabc} are the Thevenin equivalent voltage source and impedance respectively at terminal P. E_H and Z_{Habc} are the Thevenin equivalent voltage source and impedance respectively at terminal Q. Z_{abc} represents the line impedance.

Assuming that an unsymmetrical fault occurs, we can make use of the symmetrical components theory and a negative sequence network is represented as shown in Figure 4.7

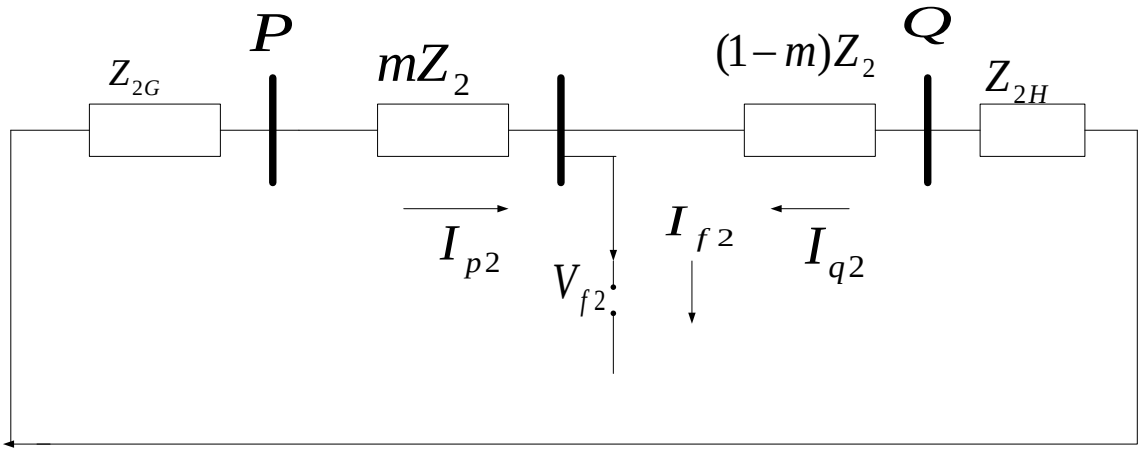

Figure 4.7 Negative Sequence Network during the fault neglecting Shunt capacitance [5]

We have

$$I_{p2} = -V_{p2} / Z_{2G} \tag{4.39}$$

$$I_{q2} = -V_{q2} / Z_{2H} \tag{4.40}$$

$$V_{p2} - mZ_2 I_{p2} = [V_{q2} - (1-m)Z_2 I_{q2}]e^{j\delta} \quad (4.41)$$

Where,

V_{p2}, I_{p2}	Negative sequence voltage and current during the fault at terminal P;
V_{q2}, I_{q2}	Negative sequence voltage and current during the fault at terminal Q;
Z_{2G}, Z_{2H}	Negative sequence source impedance at terminal P and Q;
δ	Synchronization angle between measurements at terminal P and Q;
m	Per unit fault distance from terminal P;
Z_2	Total negative sequence impedance of the line.

In the above equations, V_{p2} and V_{q2} are known based on the measurements. Then I_{p2} and I_{q2} can be obtained using Equations (4.39) and (4.40).

Solving Equation (4.41) will result in the fault location. The Detailed method is referred to the original work presented in [5]. The algorithm neglecting shunt capacitances, as presented above, has advantages of simplicity and computational efficiency. However, neglecting shunt capacitances may lead to certain errors for long lines. Consideration of shunt capacitances is discussed in [5].

The following table lists the estimated fault location for phase A to ground faults with fault resistance 5 ohms. The fault resistance value does not affect the fault location .

Table 4.1Fault location estimation

Actual fault location (p.u.)	Estimated fault location (p.u.)
0.2	0.2105
0.4	0.4124
0.6	0.6130
0.8	0.8120

It is shown from the table that quite accurate estimates have been obtained. The errors may be due to inaccuracy of Thevenin parameter estimates since the voltage and current phasors utilized are not precise.

4.8 Voltage and Current Waveforms for Different Fault Locations

The voltage and current waveforms for different fault locations are plotted which is represented in the figures in this section.

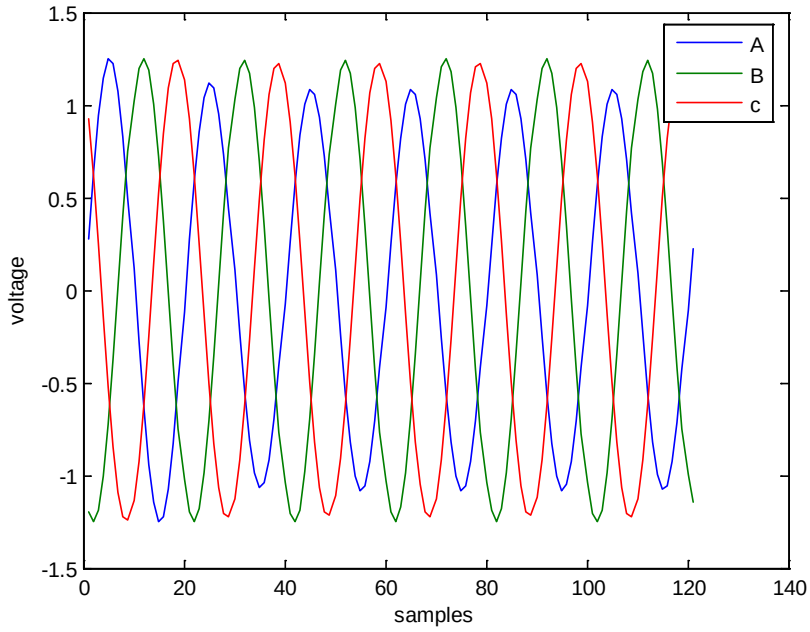

Figure 4.8(a) Voltage waveforms for a phase A to ground fault with a fault location of 0.2 p.u

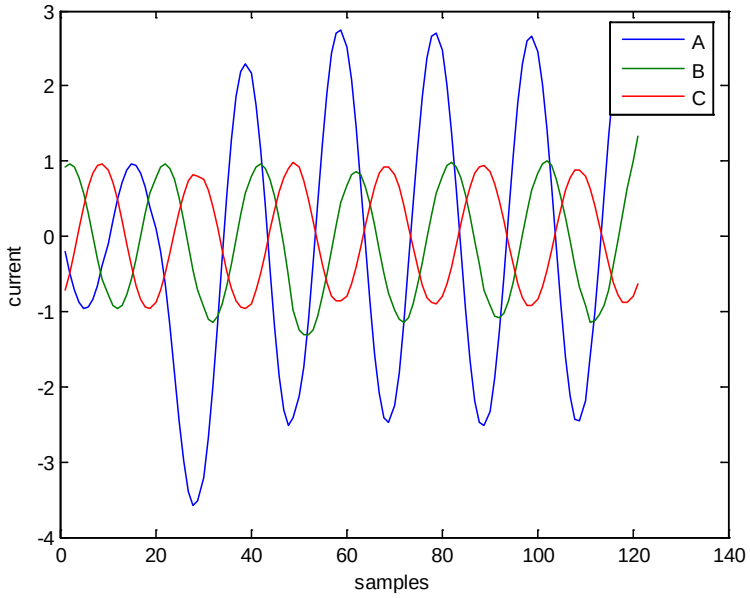

Figure 4.8(b) Current waveforms for a phase A to ground fault with a fault location of 0.2 p.u

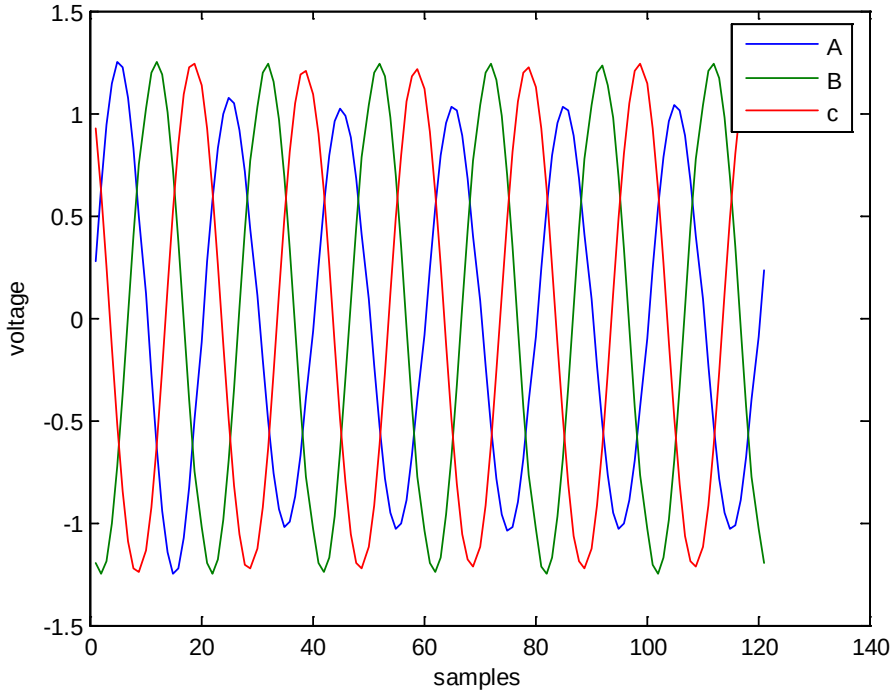

Figure 4.9(a) Voltage waveforms for a phase A to ground fault with a fault location of 0.4 p.u

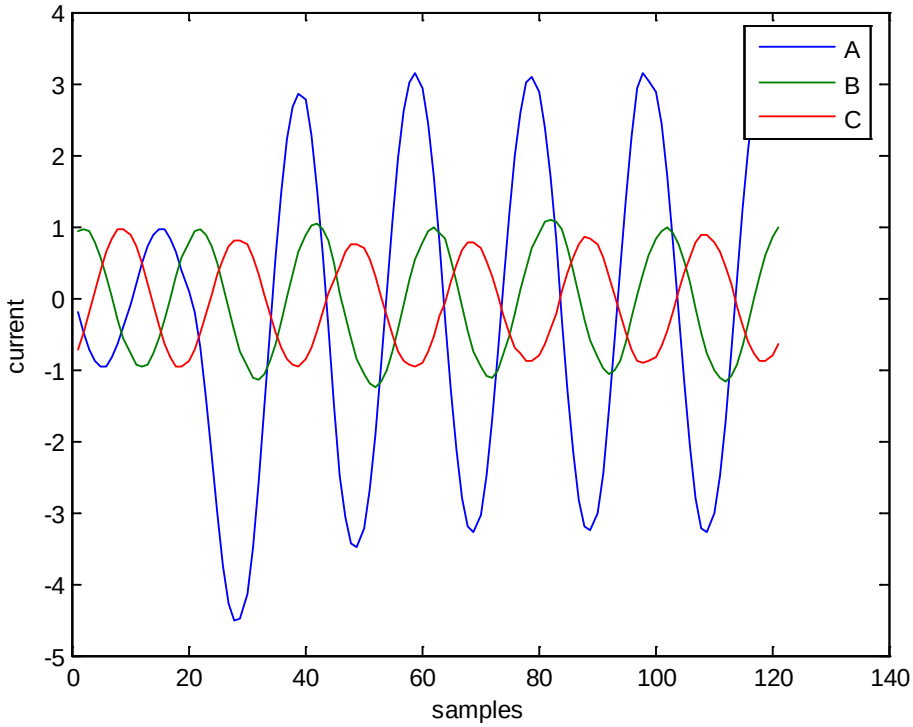

Figure 4.9(b) Current waveforms for a phase A to ground fault with a fault location of 0.4 p.u

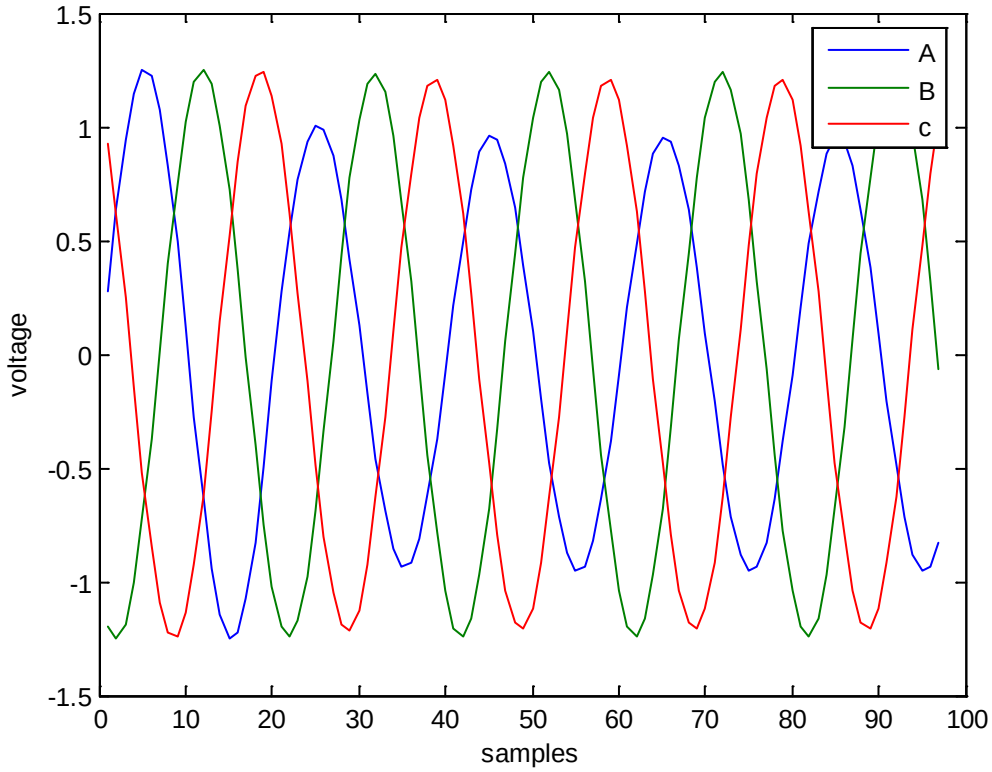

Figure 4.10(a) Voltage waveforms for a phase A to ground fault with a fault location of 0.6 p.u

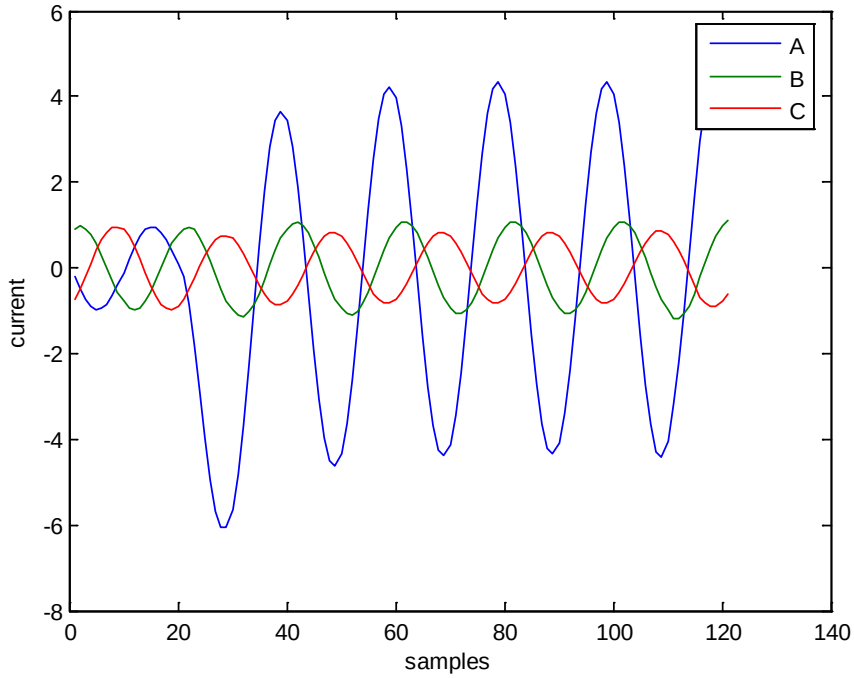

Figure 4.10(b) Current waveforms for a phase A to ground fault with a fault location of 0.6 p.u

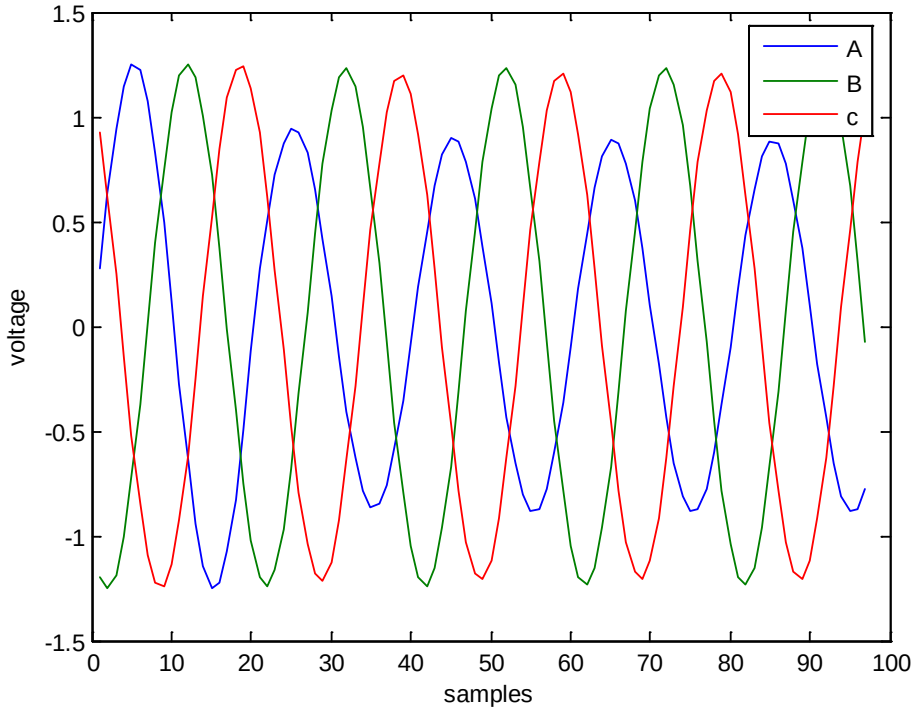

Figure 4.11(a) Voltage waveforms for a phase A to ground fault with a fault location of 0.7 p.u

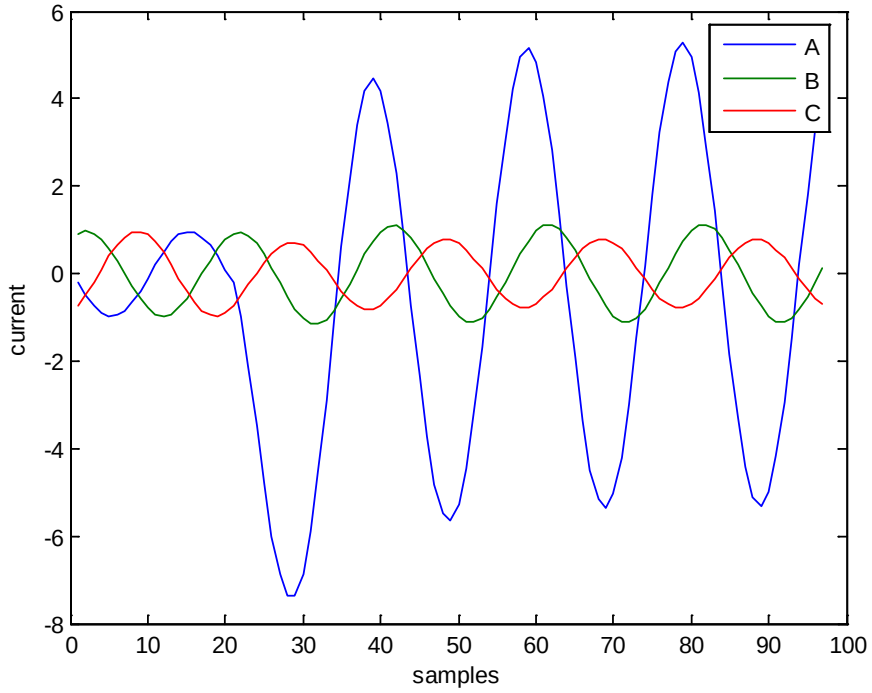

Figure 4.11(b) Current waveforms for a phase A to ground fault with a fault location of 0.7 p.u

5. Conclusion

The main objectives of this thesis were Thevenin parameters estimation, determining the maximum power that can be transferred and the estimation of fault location. In Chapter 3, we made use of MATLAB SIMULINK® to simulate the power system model that has been used in this Thesis. The results yielded the values of Thevenin equivalent parameters. These in turn were used to calculate the maximum power that can be transferred to the load bus under different conditions. In Chapter 4 we used the values of the Thevenin parameters for fault location. The results obtained confirm the available results of the algorithms that have been used.

Bibliography

[1] M H Haque, *On-line monitoring of maximum permissible loading of a power system within voltage stability limits* IEE Proceedings on Generation, Transmission and Distribution, Vol. 150, No. 1, January 2003

[2] Prabha Kundur, *Power System Stability and Control*, McGraw-Hill, 1994

[3] Prabha Kundur, John Paserba, Venkat Ajjarapu, Göran Andersson, Anjan Bose, Claudio Canizares, Nikos Hatziargyriou, David Hill, Alex Stankovic, Carson Taylor, Thierry Van Cutsem, and Vijay Vittal, *Definition and Classification of Power System Stability*, IEEE Transactions on Power Systems, Vol. 19, No. 2, May 2004

[4] D P Kothari, I J Nagrath, *Modern Power System Analysis*, McGraw-Hill, 2003

[5] Yuan Liao, *Fault Location Utilizing Unsynchronized Voltage Measurements during Fault*, Electric Power Components and Systems, Vol.34, pp: 1283–1293, 2006

[6] B Milosevic and Miroslav Begovic, *Voltage-Stability Protection and Control Using a Wide-Area Network of Phasor Measurements*, IEEE Transactions on Power Systems, Vol. 18, No.1, February 2003

[7] IEEE Special Publication 907H0358-2-PWR, *Voltage stability of Power Systems: Concepts, Analytical Tools and Industry Experience*, 1990

[8] B. M. Weedy, B. J. Cory, *Electric Power Systems*, John Wiley & Sons, 1998

[9] Khoi Vu, Miroslav M. Begovic, Damir Novosel, Murari Mohan Saha, *Use of Local Measurements to Estimate Voltage-Stability Margin*, IEEE Transactions on Power Systems, Vol. 14, No. 3**,** August 1999

[10] Matlab Student Version 7.0.0 19920 (R14) SimPower Systems May 2004

[11] Tamer Kawady and Jürgen Stenzel, *A Practical Fault Location Approach for Double Circuit Transmission Lines Using Single End Data*, IEEE Transactions on Power Delivery, Vol. 18, No. 4, October 2003

[12] Yuan Liao, *Fault Location for Single-Circuit Line Based on Bus-Impedance Matrix Utilizing Voltage Measurements*, IEEE Transactions on Power Delivery, Vol. 23, No. 2, April 2008

[13] Yuan Liao, *Transmission Line Fault Location Algorithms without Requiring Line Parameters*, Electric Power Components and Systems, Vol. 33, No. 10, October 2005

[14] Y Liao and S Elangovan, *Improved symmetrical component-based fault Distance estimation for digital distance protection*, IEE Proceedings on Generation, Transmission and Distribution, Vol. 145, No. 6, November 1998

[15] J J Grainger and W D Stevenson Jr., *Power System Analysis*, McGraw Hill, 1994

Vita

Mohammad Museb Iftakhar was born in Karimnagar, Andhra Pradesh, India on December 14th, 1985. He received his Bachelor of Engineering degree in Electrical and Electronics Engineering in 2006 from Osmania University, Hyderabad, India. He worked as a Research Assistant in spring 2007 in the Power Systems Research Group at the University of Kentucky, Lexington, Kentucky, U.S.A.

Mohammad M Iftakhar